Use of FLIM-FRET and FCS to monitor viral proteins and their interactions

Yves MELY

UMR 7213 CNRS, Laboratoire de Biophotonique et Pharmacologie

ILLKIRCH, France

1st School on Advanced Fluorescence Imaging (ADFLIM), Moscow, Russia, December 12-14, 2016

Why measuring fluorescence lifetimes?

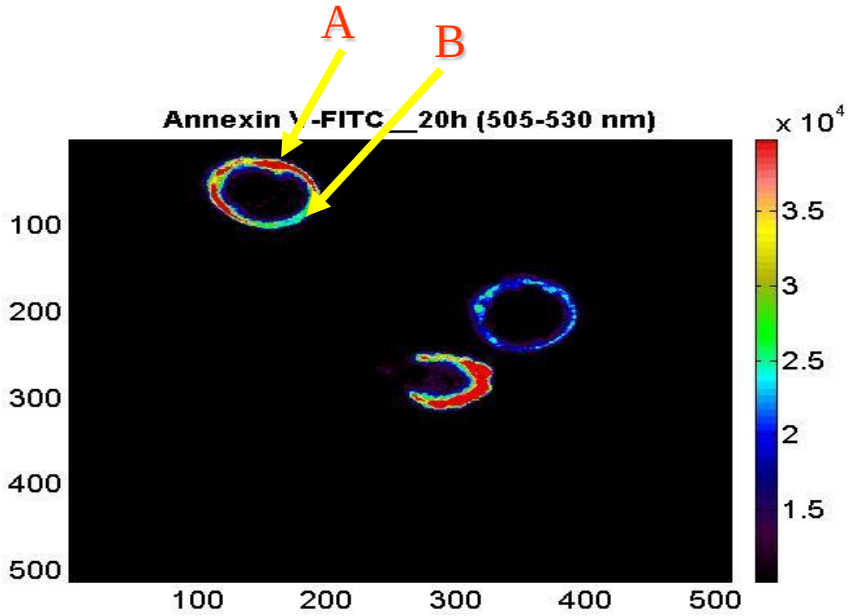

Fluorescence intensities depend on instrumentation and probe concentration

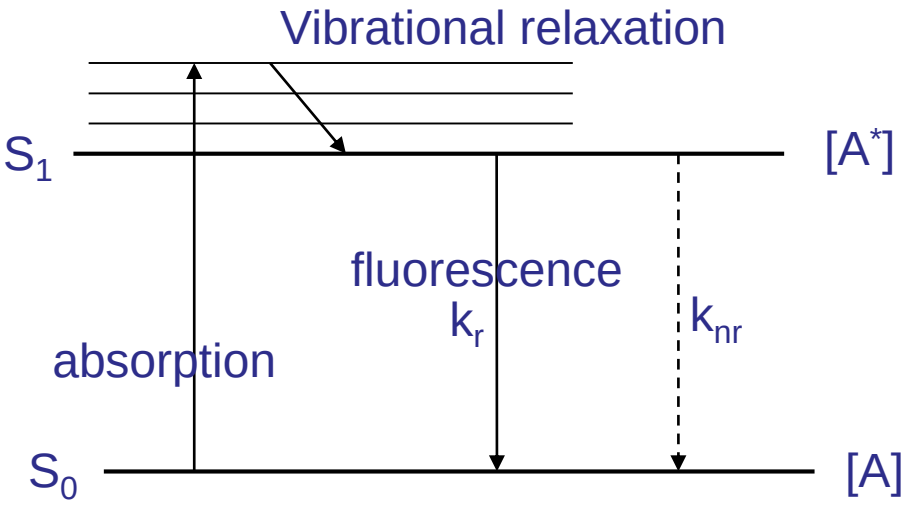

Lifetime τ = average time spent in the excited state = $1/(k_r+k_{nr})$

Fluorescence lifetimes are independent of the instrumentation and probe concentration

$$I(t) = I_0 \sum_i \alpha_i \exp(-t/\tau_i)$$

10 ps < τ < 100 ns. Usually: 1-5 ns.

Fluorescence lifetime measurements in solutions

Time Correlated Single Photon Counting Technique

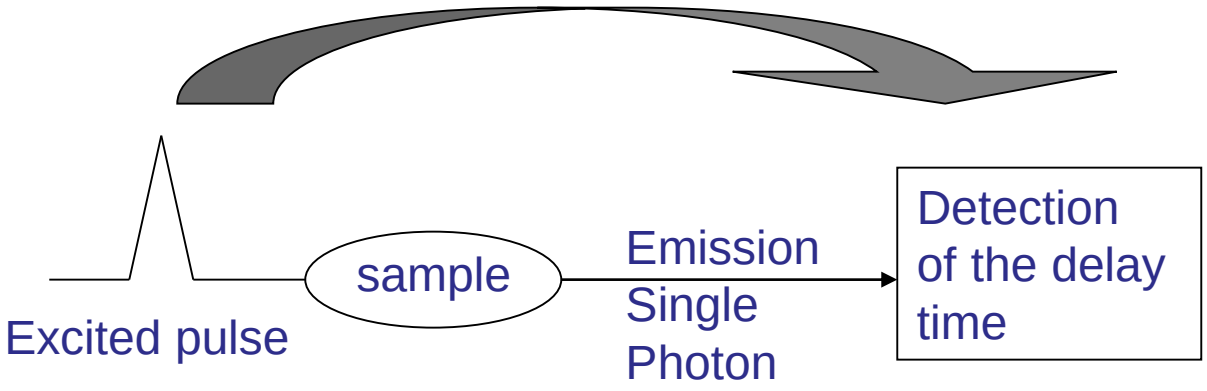

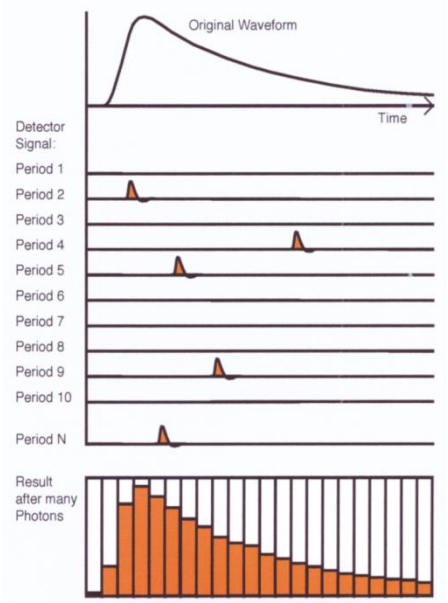

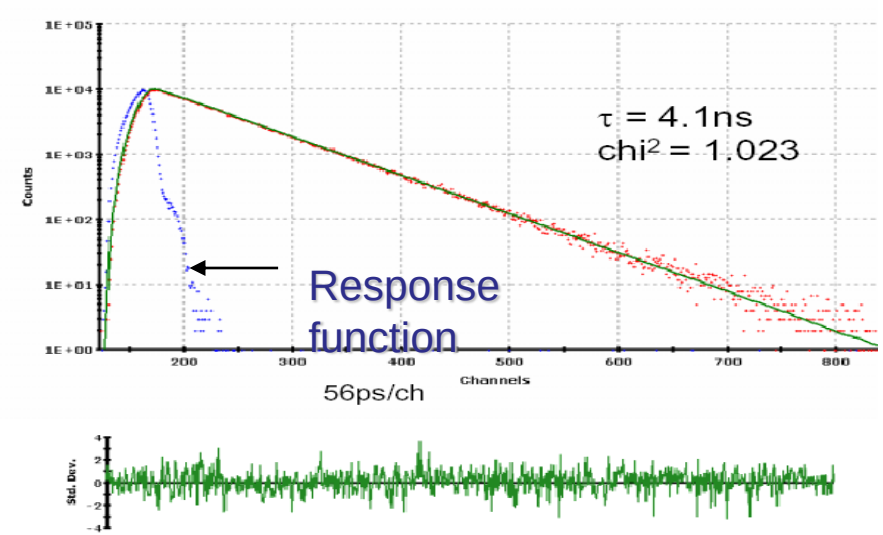

Very good statistics: 10^6 photons: up to 5 lifetimes

Fluorescence lifetime imaging Microscopy(FLIM)

Lifetimes are measured for each pixel of the microscope image.

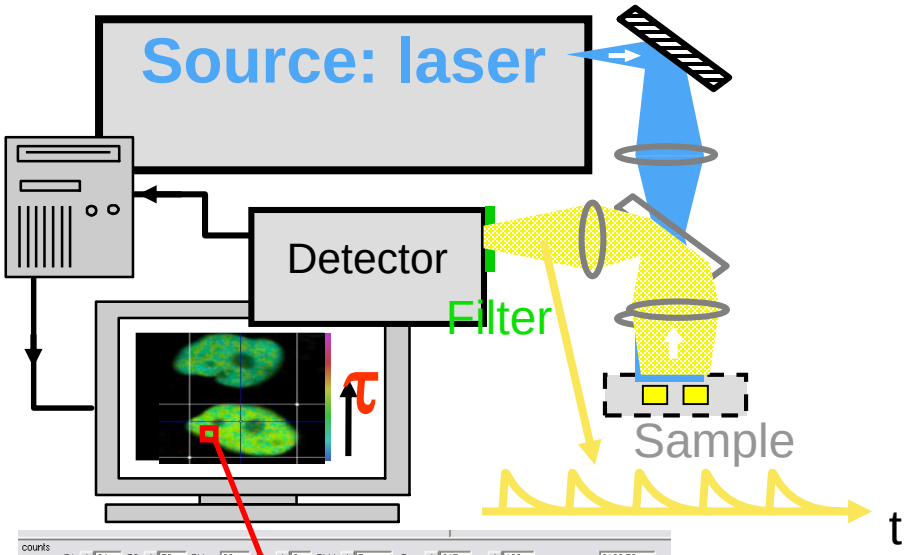

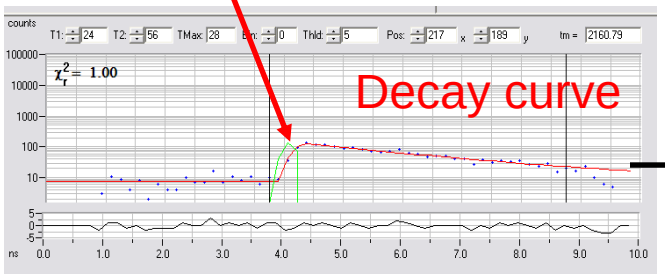

Lifetime

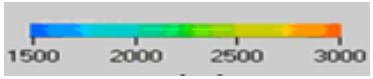

Confocal microscopy or two photon microscopy. Low number of photons ($< 10^3$ photons): usually one or two lifetimes $\rightarrow$ mean lifetime.

FLIM: measurements of physico-chemical parameters

Intracellular pH: C-SNAFL2 probe.

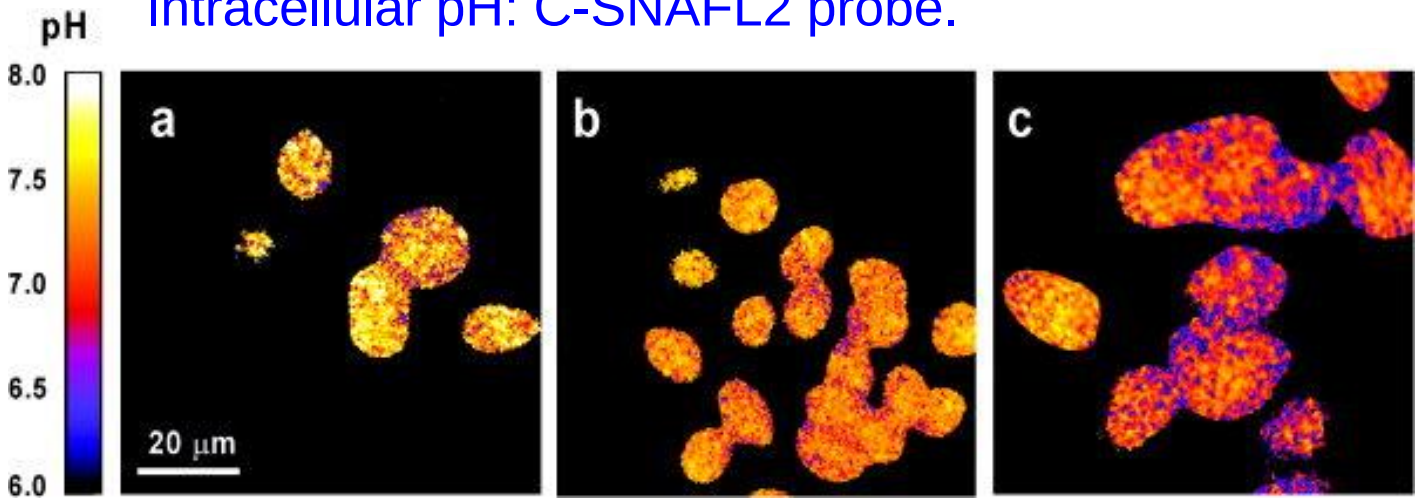

Cellules 3T3 Cellules CHO Cellules MCF-7

Cytometry A. 2003, 52:77-89

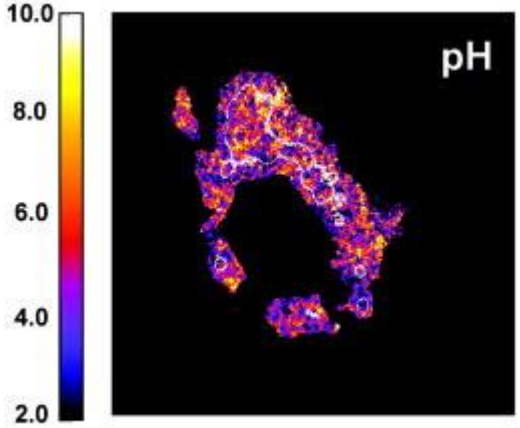

Lysosensor-DND 160: acidic compartments

Intracellular calcium and oxygen concentrations could also be monitored.

FRET-FLIM: monitoring molecular interactions

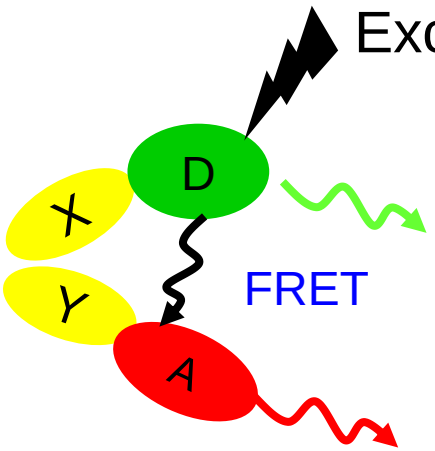

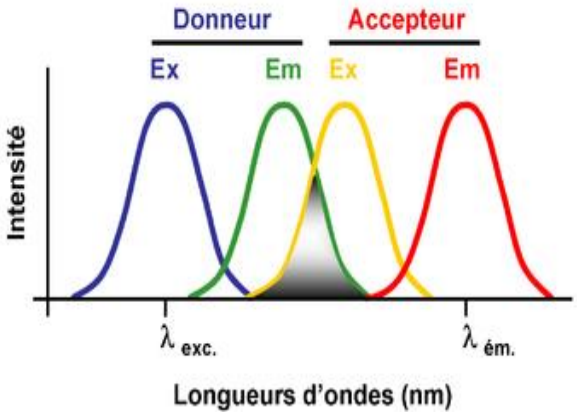

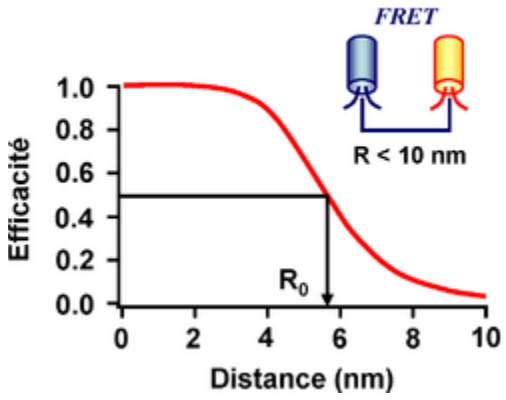

$$E = \frac{R^{-6}}{R^{-6} + R_0^{-6}}$$

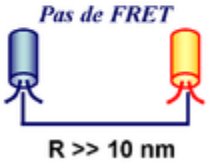

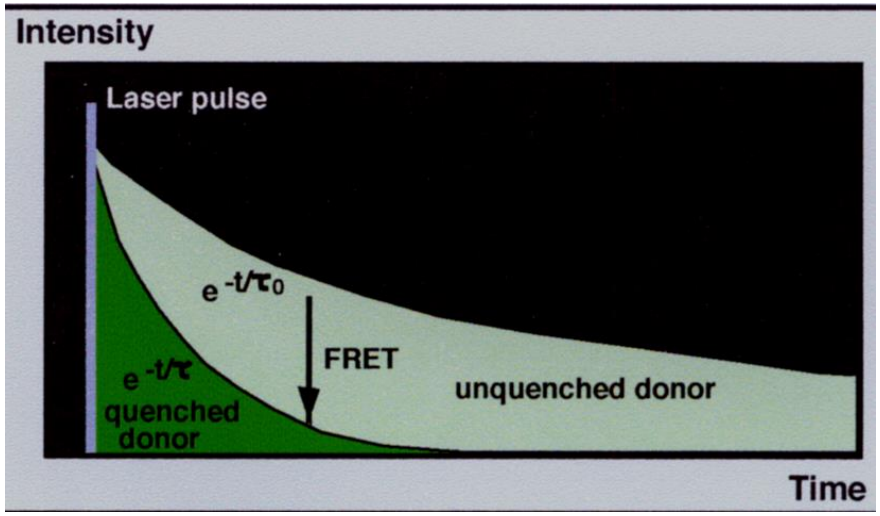

τ value depends on the interchromophore distance

Fluorescence lifetime decreases when FRET → proof of molecular interaction.

HIV-1 assembly and budding

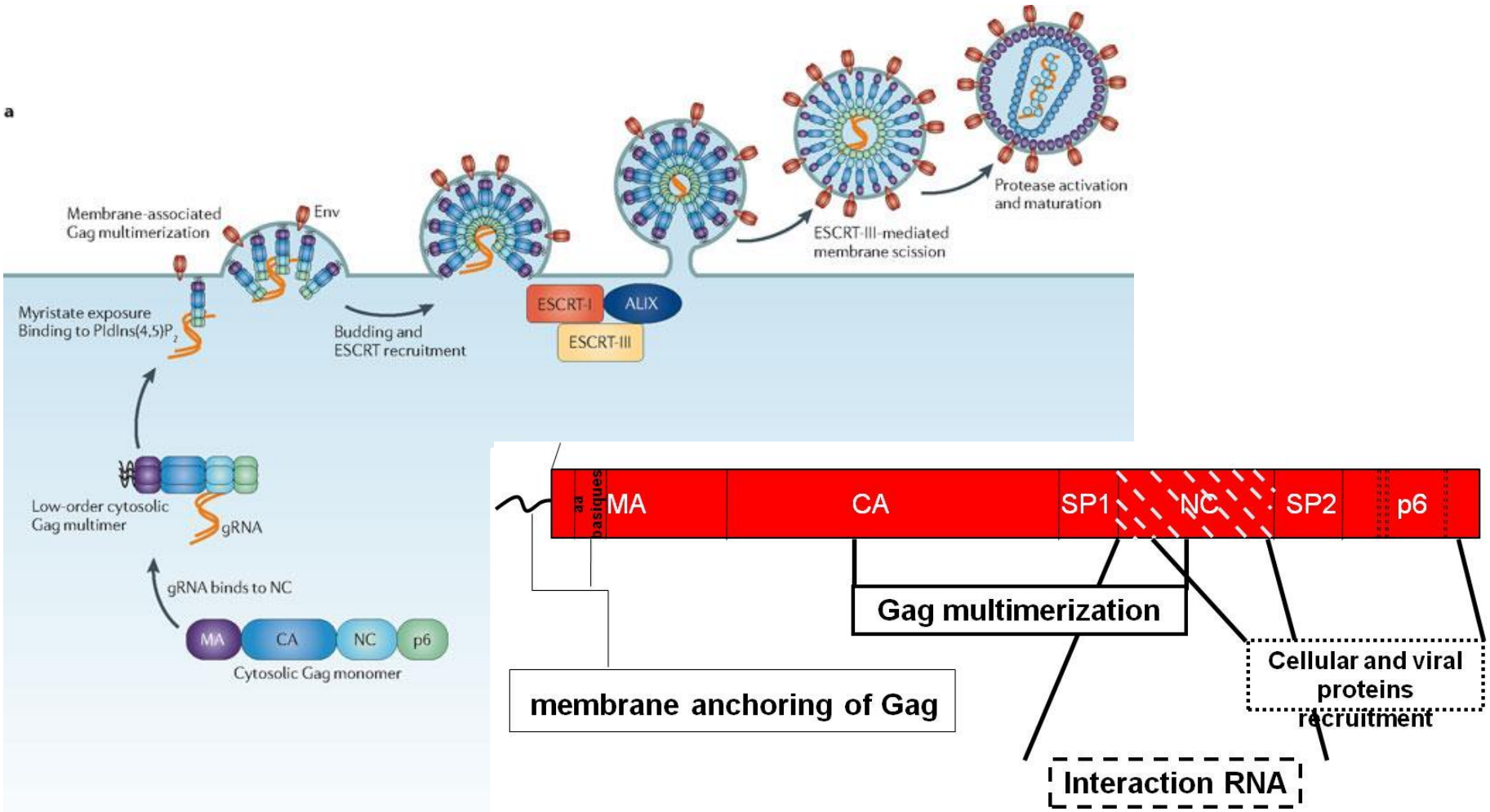

Serrano & Neil, Nature Reviews Microbiol, 2011

What is the oligomeric state of Gag in the cytoplasm? Can we visualize the Gag oligomerisation in cells? What is the role of NC domain in this oligomerization?

Insertion of a fluorescent reporter in the HIV-1 Gag polyprotein

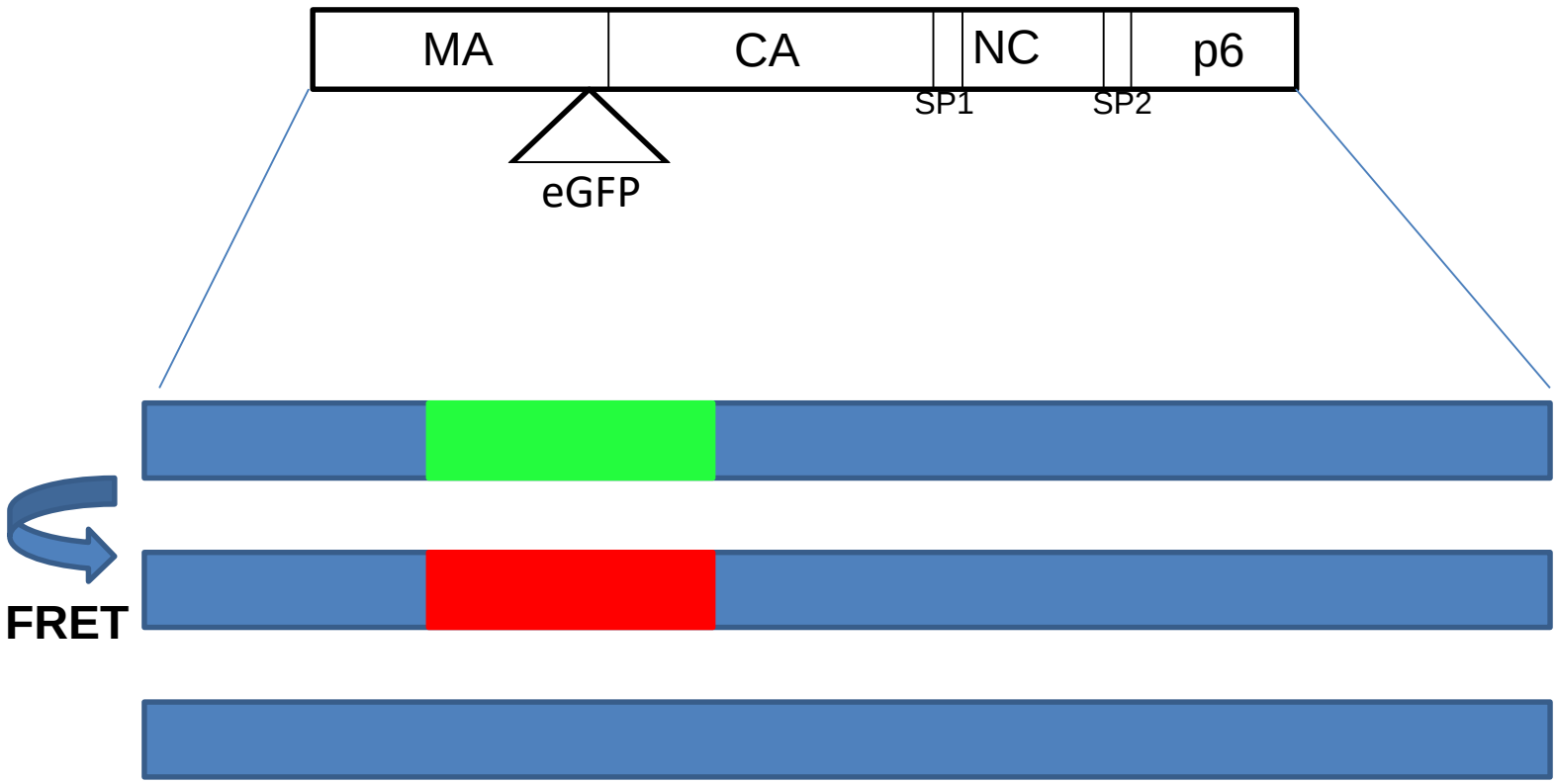

Combination of Gag/Gag-eGFP/Gag-mcherry (70/10/20) was shown to not hinder the assembly process.

Muller et al, 2006, Fritz et al, 2010

FLIM imaging

One component analysis

12 h

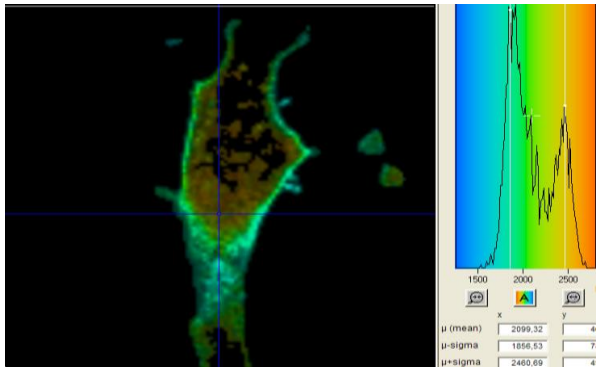

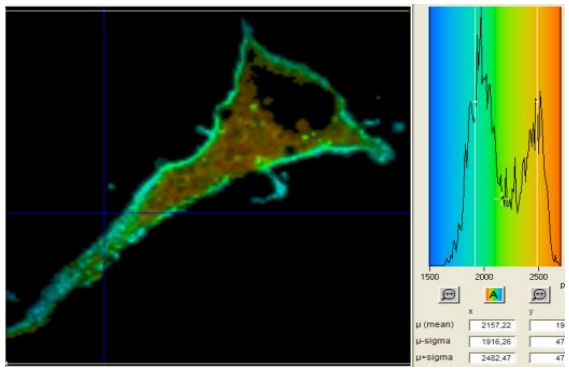

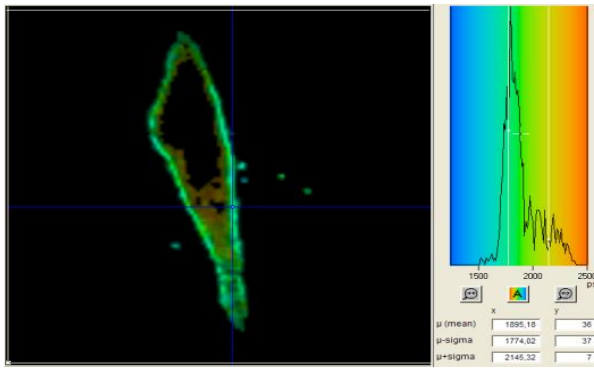

24 h

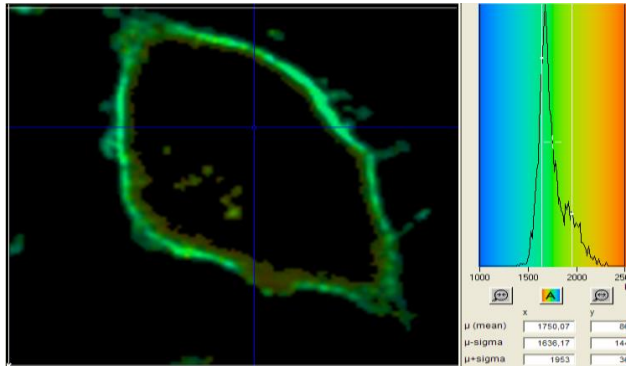

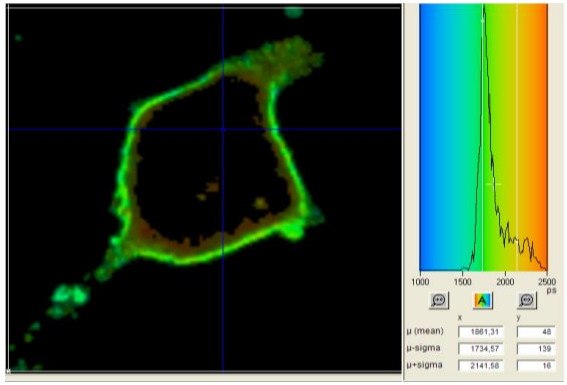

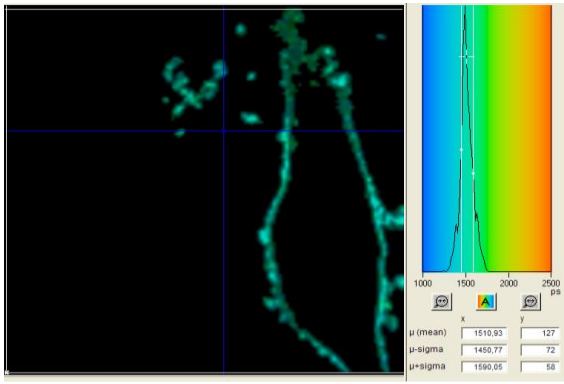

Clear time dependence of the localization of the Gag proteins, with an accumulation at the PM. Two populations: one with the eGFP lifetime → Gag monomers or small oligomers, one with $\tau \leq 2$ ns: Gag oligomers.

De Rocquigny et al, 2014, Virus Res, 2014
El Meshri et al, J Mol Biol, 2015

FLIM imaging: two component analysis

Short component (2.4 ns fixed)

12h

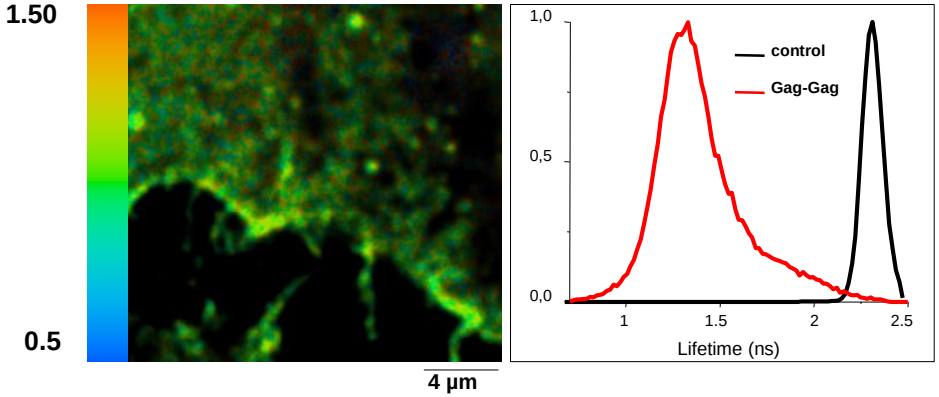

At 12h, short lifetime 1.45±0.1 ns (41% FRET) is homogeneously distributed within the cell

24h

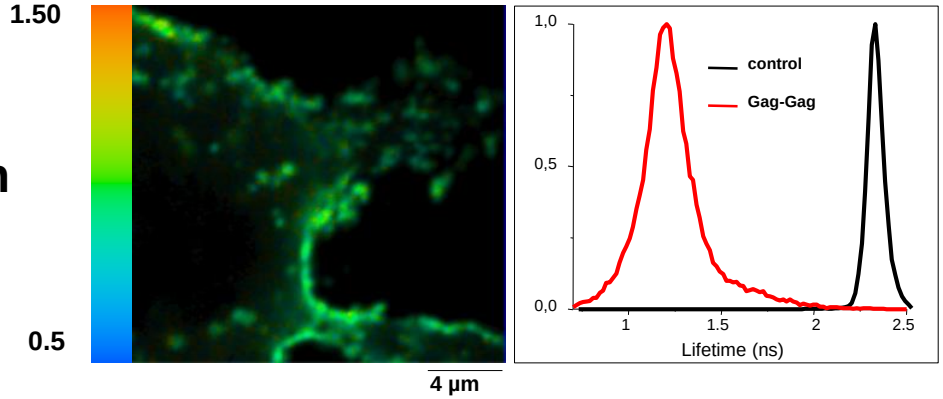

At 24h, short lifetime 1.2±0.1 ns (50% FRET) is concentrated close to and at the PM

Closely packed Gag oligomers form in the cytoplasm and accumulate with time at the PM. Gag molecules further compact and/or increase in size at the membrane.

FLIM imaging: two component analysis

Amplitude of the short component

12h

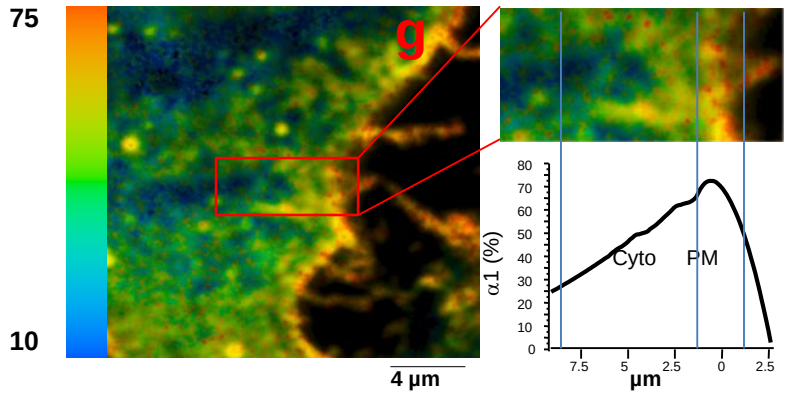

Fraction of the FRET component increases from 20 to 75 % from the cytoplasm to the PM: spatial enrichment in the population of oligomers towards the PM

24h

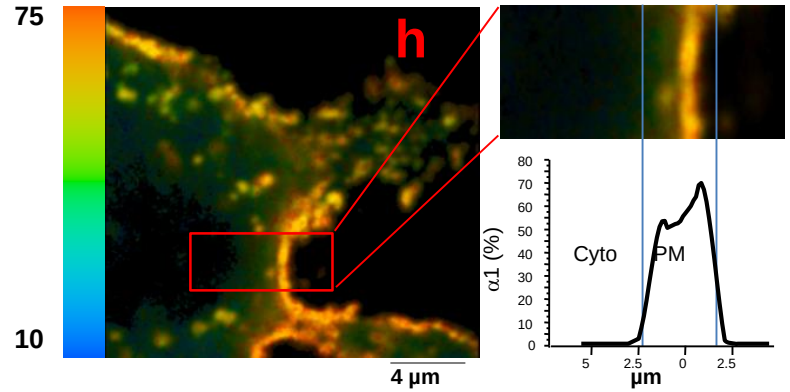

Short-lived component represents 75 % at the PM → almost all Gag molecules undergo FRET at the PM

Formation of Gag oligomers is initiated in the cytoplasm. These oligomers progressively assemble on their way to the PM, where they accumulate.

Prediction of FRET efficiency at the PM

Short component (2.4 ns fixed)

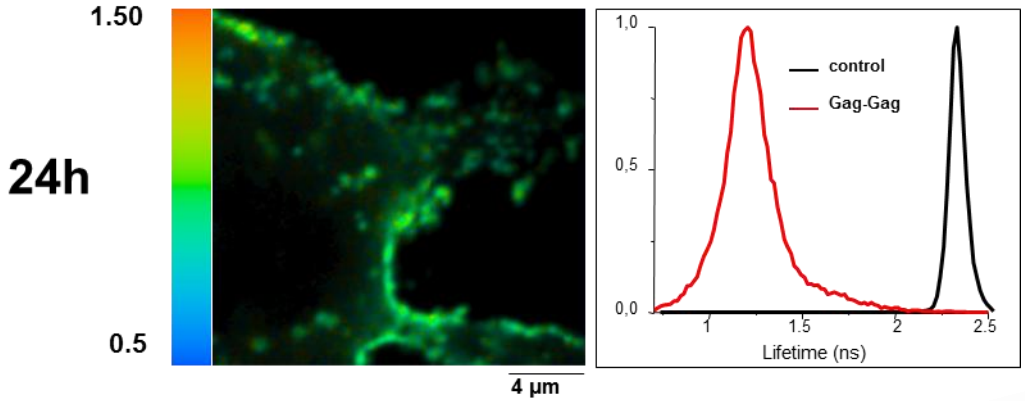

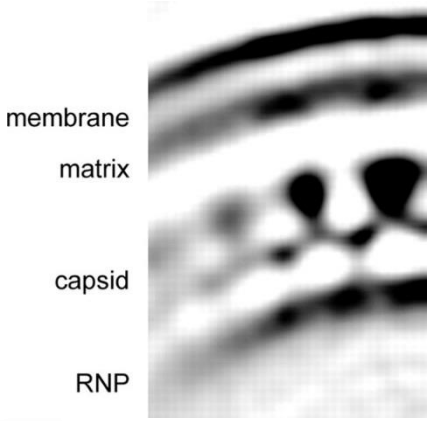

Organisation of Gag at the PM

Briggs J A G et al. PNAS, 2014

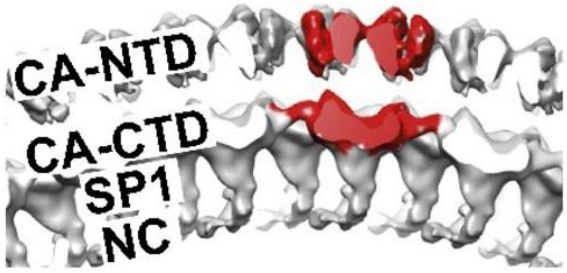

Bharat et al. PNAS 2014

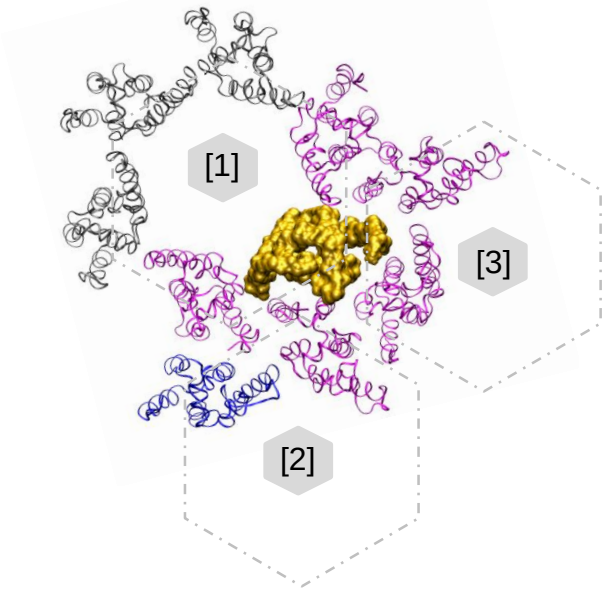

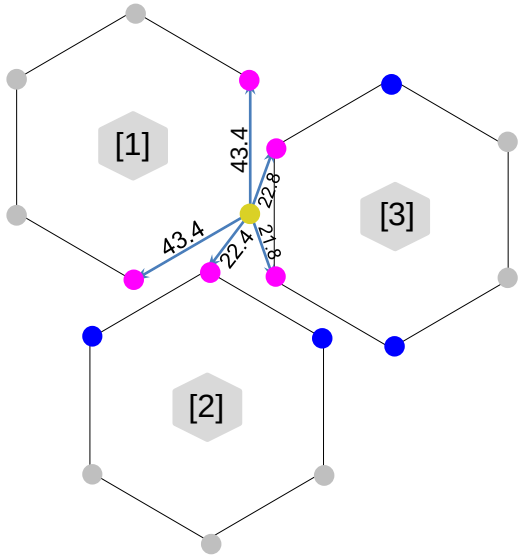

Assuming a minimum inter-FP distance of 40Å, and resampling Gag-eGFP, Gag-mCherry and wt Gag positions according to their respective concentrations (10%, 20% and 70%, respectively), we found an average FRET of 52%, in line with the experimental FRET (50%).

Role of NC domain in Gag assembly

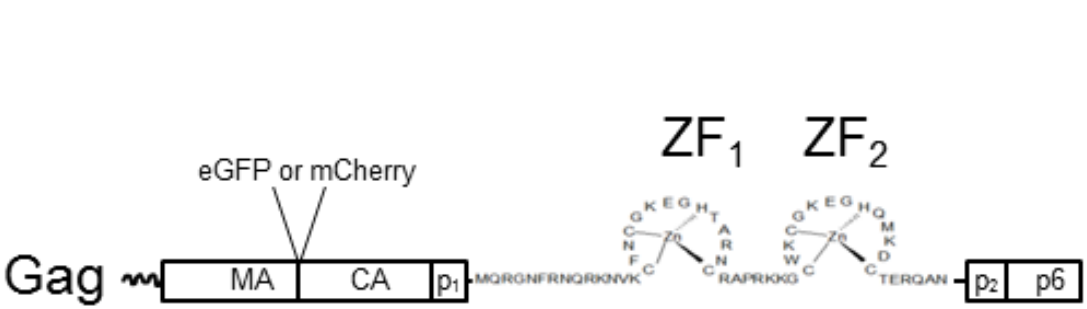

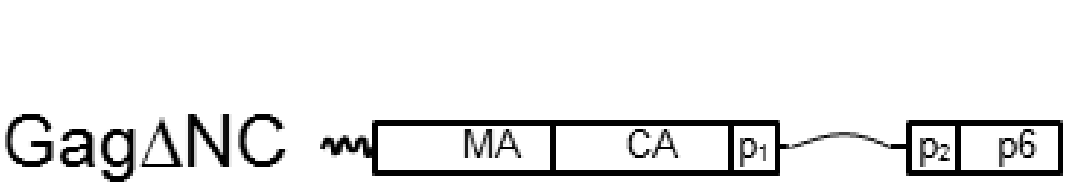

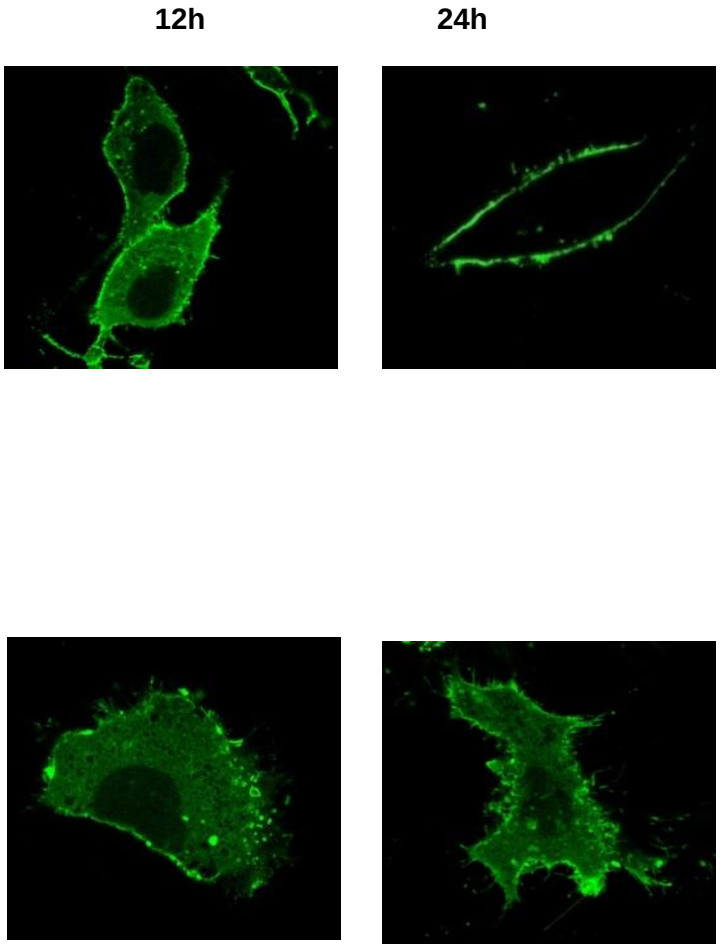

Deletion of the NC domain strongly decreases the accumulation of Gag at the PM.

Role of NC in Gag assembly

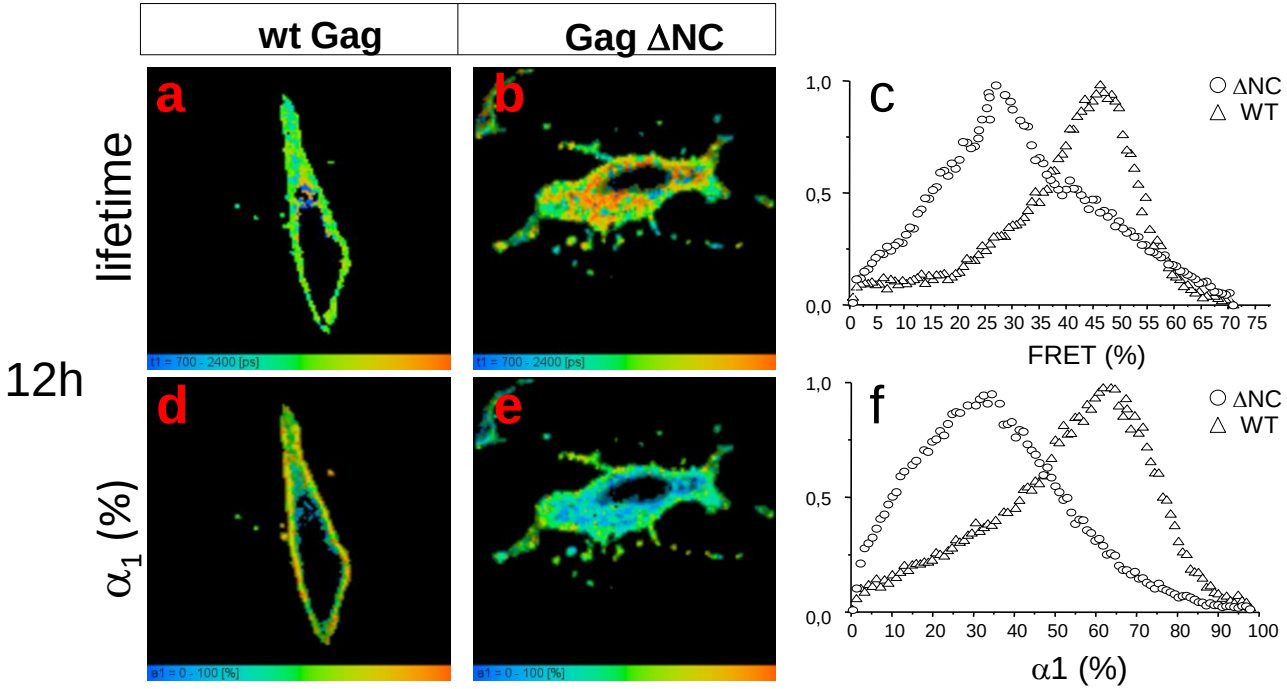

FRET shifted from 41% for wt Gag to 29 % for GagΔNC

FRET population decreased by 2-fold

Less oligomers are formed with GagΔNC and the oligomers are less packed. As NC deletion prevents binding of Gag to RNAs, the key role of NC is likely related to its ability to scaffold with RNA the packing and oligomerization of Gag.

Role of the two zinc fingers of NC in Gag assembly

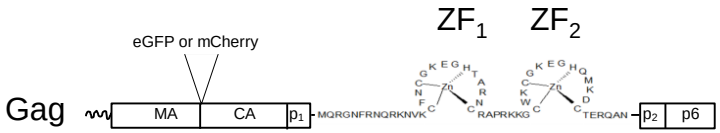

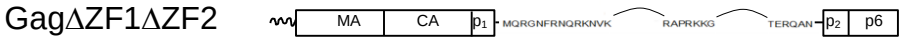

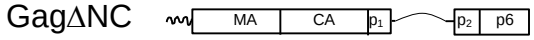

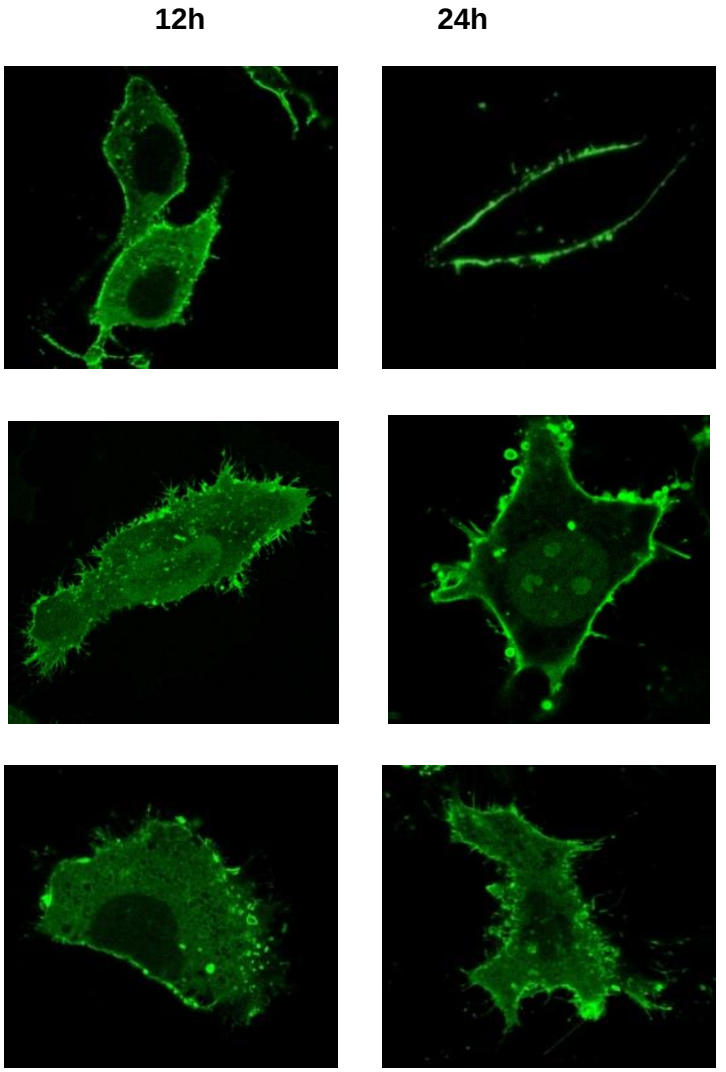

The decrease of Gag at the PM is less dramatic with the GagΔZF1ΔZF2 mutant as compared to GagΔNC → the basic domains flanking the ZFs play a role in the trafficking of Gag to the PM, likely by interacting with the cytoskeleton or motor proteins.

Role of the two zinc fingers of NC in Gag assembly

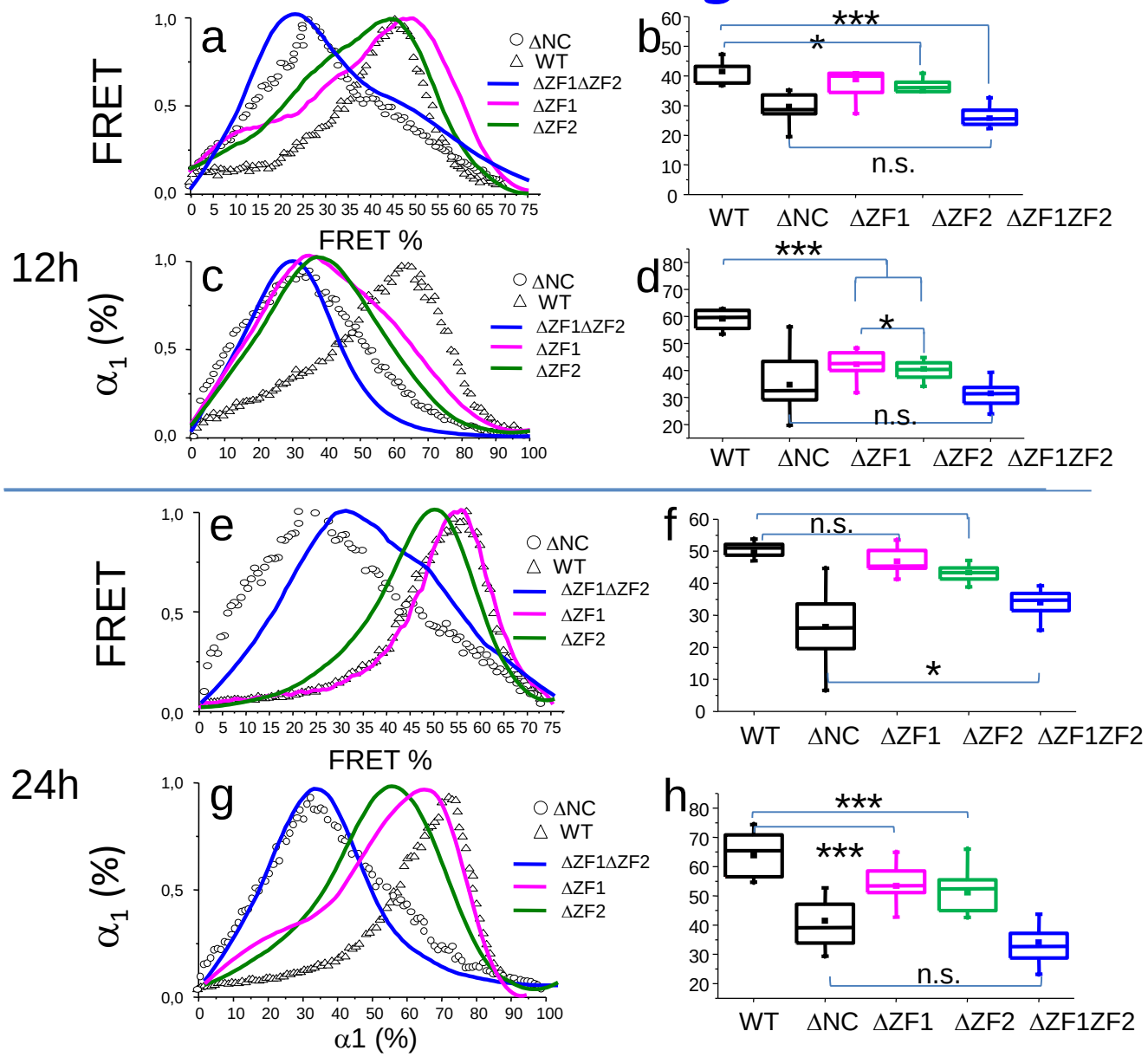

Deletion of the two fingers provides the same changes as deletion of the full NC domain in terms of FRET population and oligomer packing.

Conclusions I: Proposed model for Gag assembly

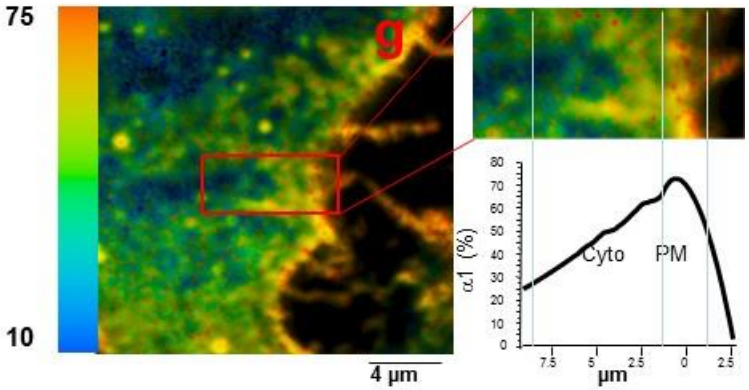

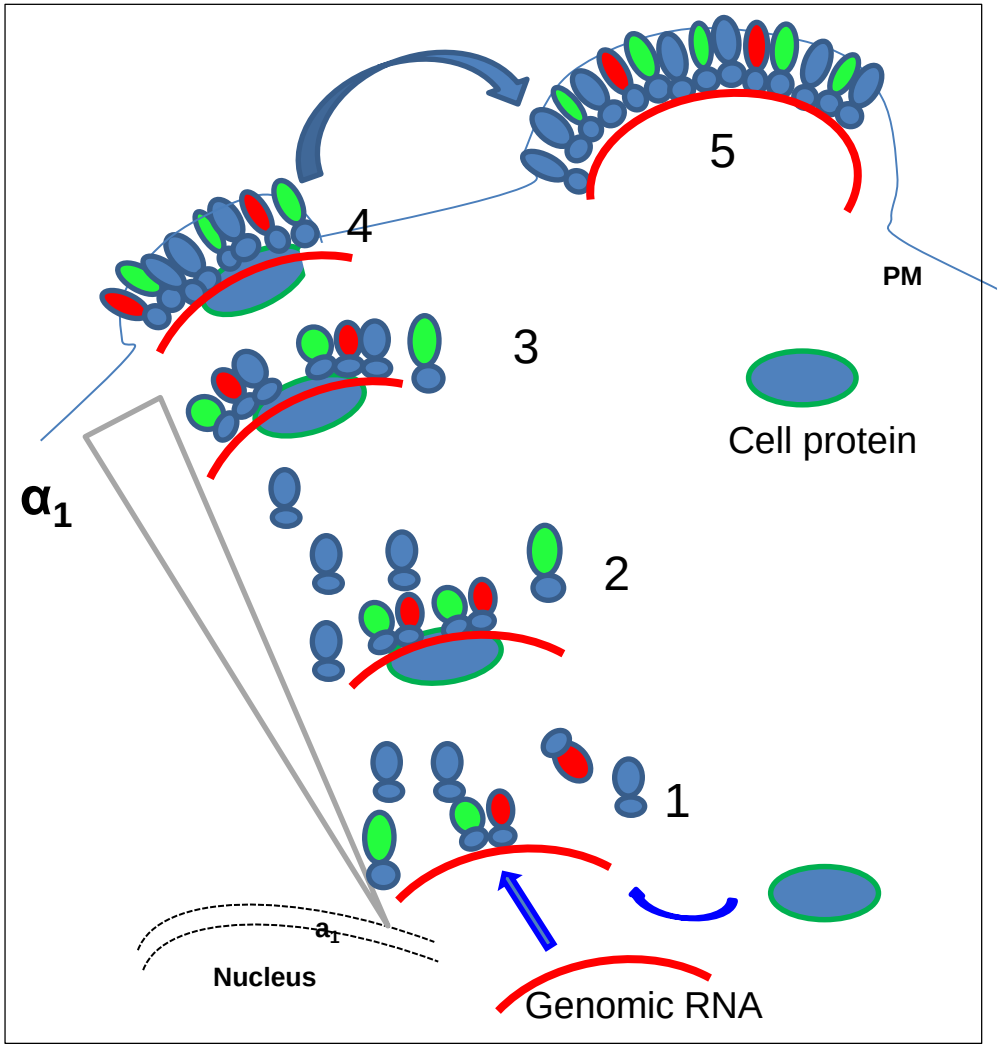

Oligomers form in the cytoplasm. Number of the oligomers progressively increases when they approach the PM. RNA binding is required for efficient Gag oligomerization, and close packing of the Gag molecules inside oligomers. Cellular partners are needed

Oligomerization of HIV-1 Vpr

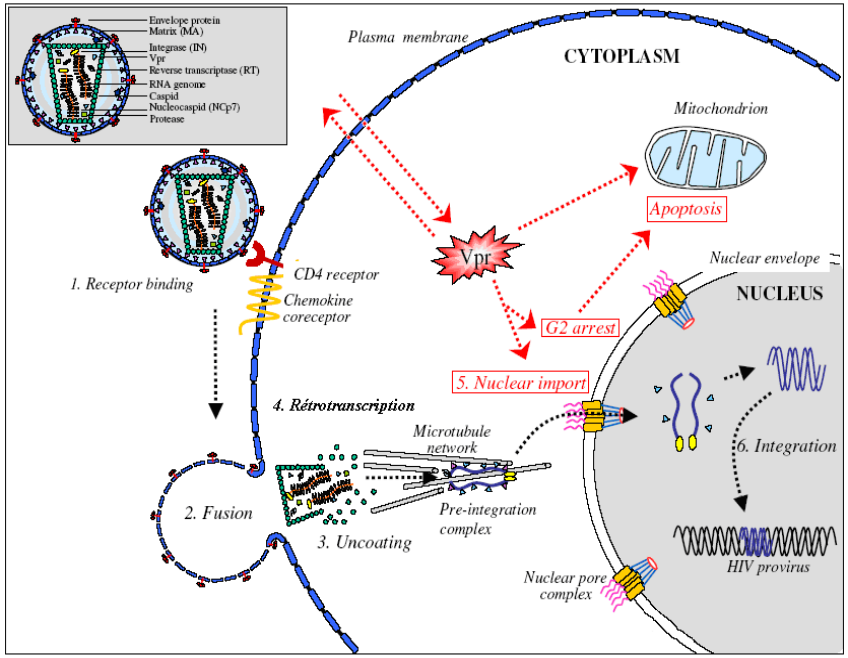

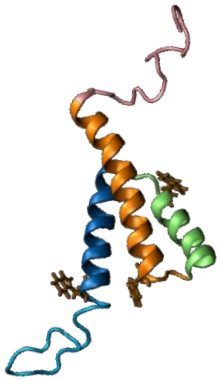

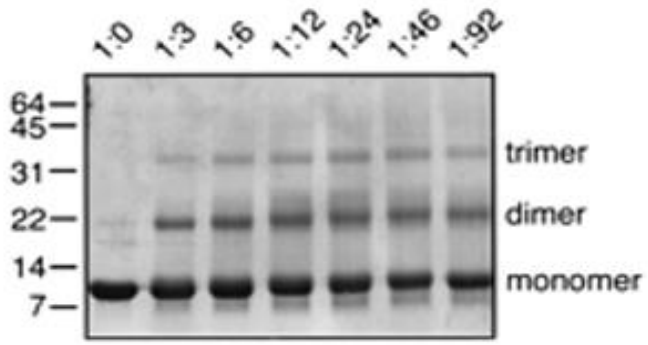

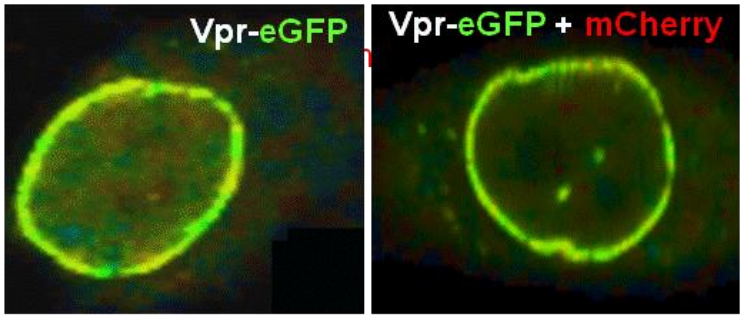

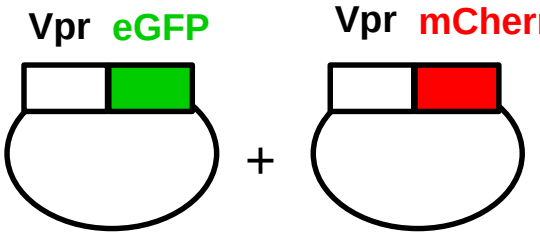

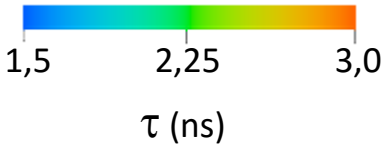

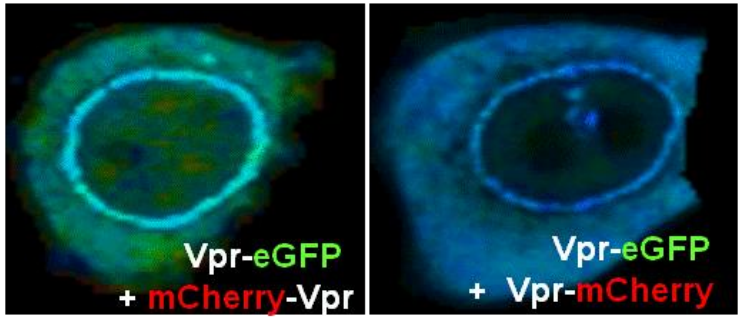

E=15% E=23%

Vpr oligomerizes in the whole cell

Fritz et al, Retrovirology, 2008

Determinants of Vpr oligomerization

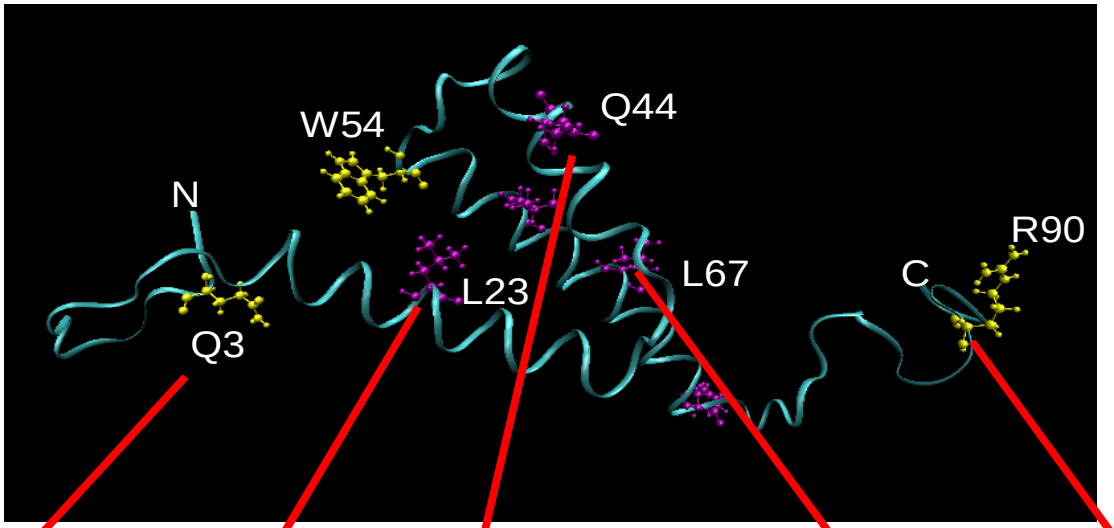

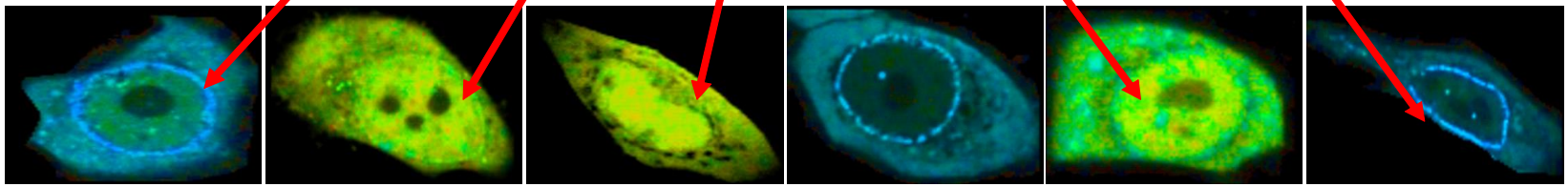

Q3R N-terminal	L23F 1st helix	ΔQ44 2nd helix	W54G Outside helix	L67A 3rd helix	R90K C-terminal

- Vpr oligomerization and binding to the nuclear membrane are correlated

-Vpr oligomerization is critically dependent on residues in the α-helices

- What's about the stoichiometry?

Fritz et al, Retrovirology, 2008

Fluorescence correlation spectroscopy

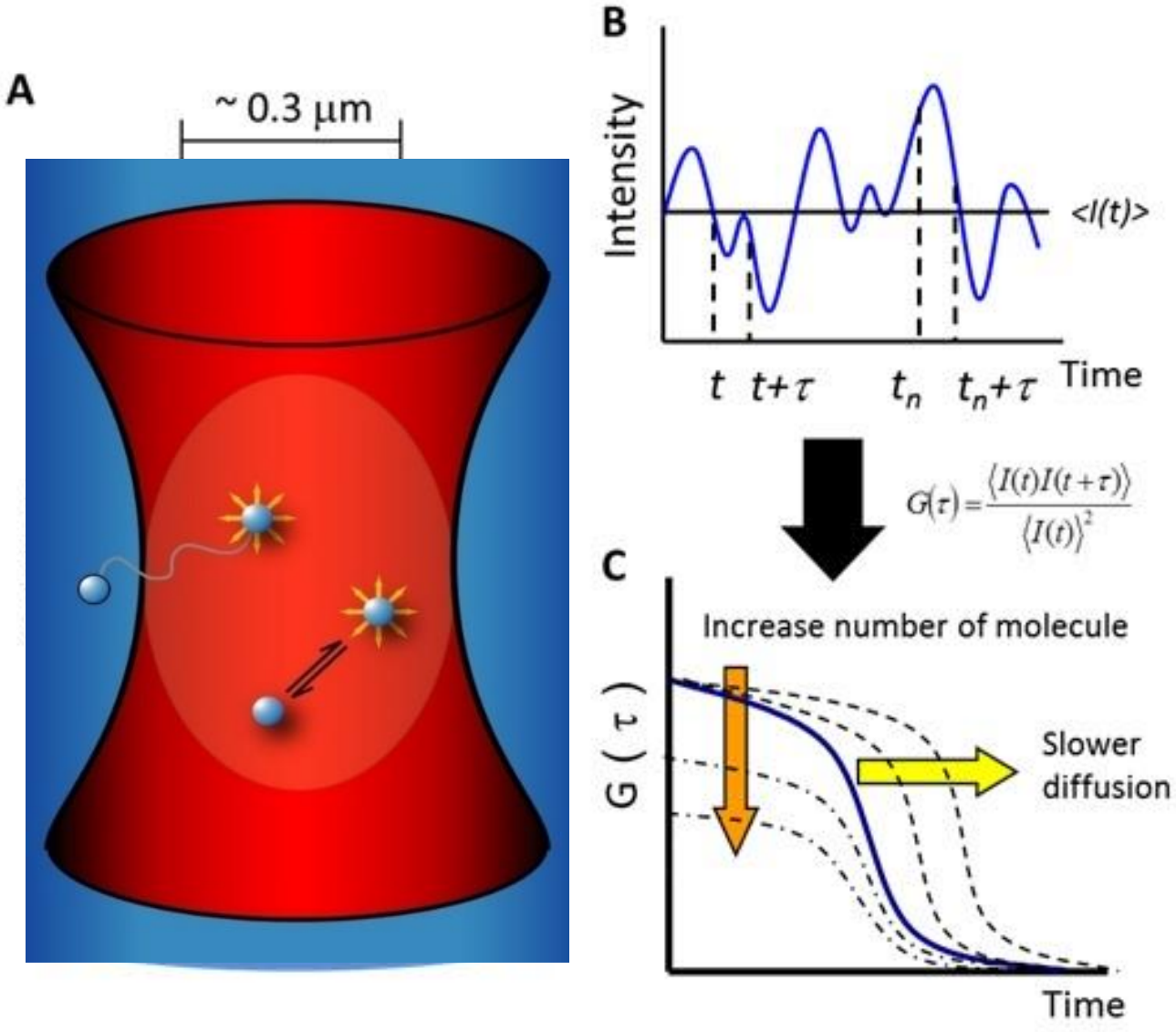

Stoichiometry of Vpr oligomers: FCS

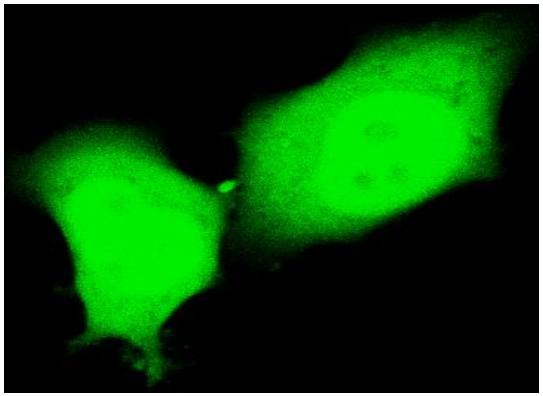

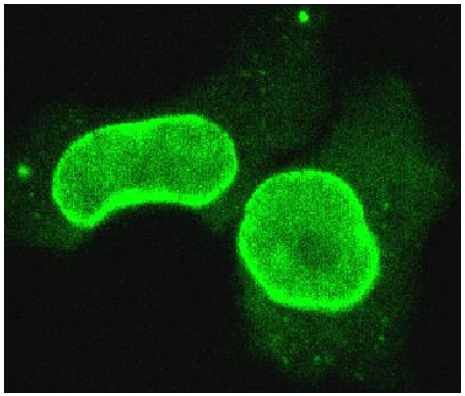

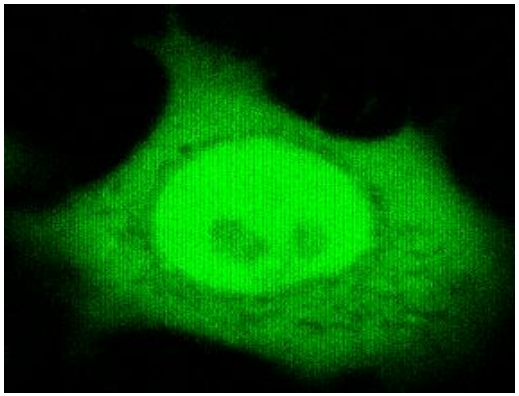

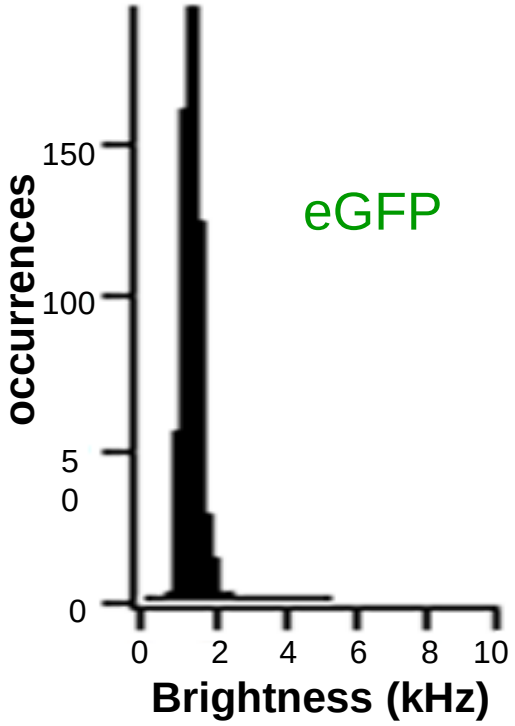

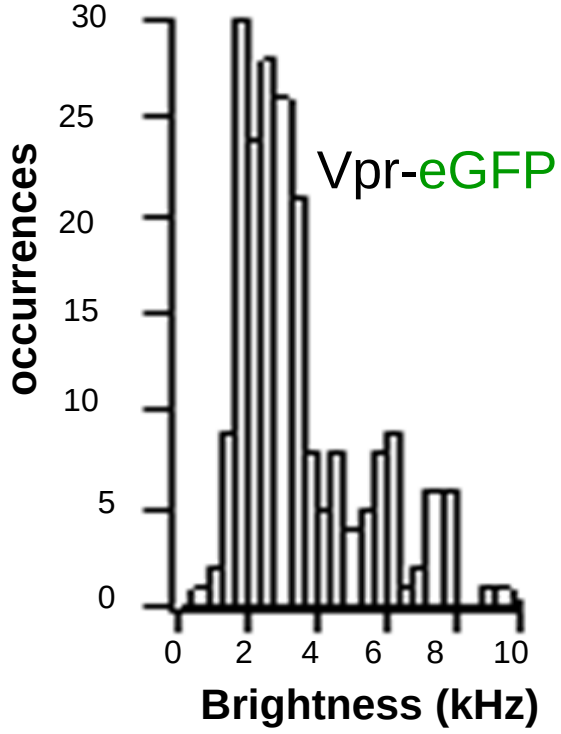

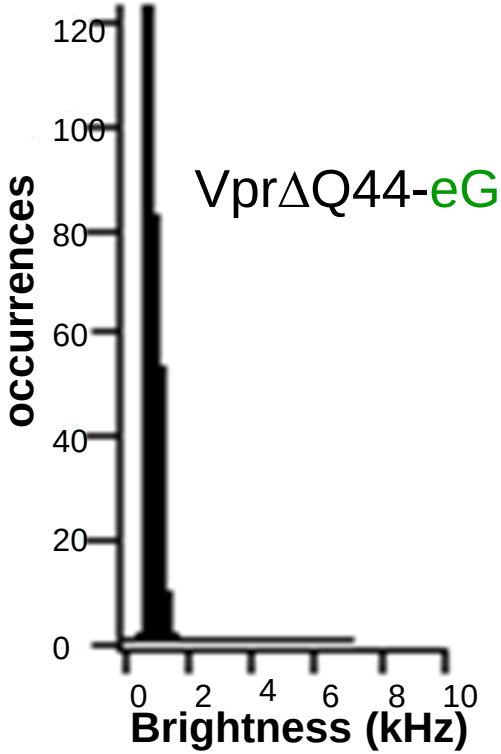

Vpr forms mainly dimers and trimers in the cytoplasm. The Vpr mutant is monomeric.

Fritz et al, Retrovirology, 2008

How is Vpr recruited in the viral particle, during assembly?

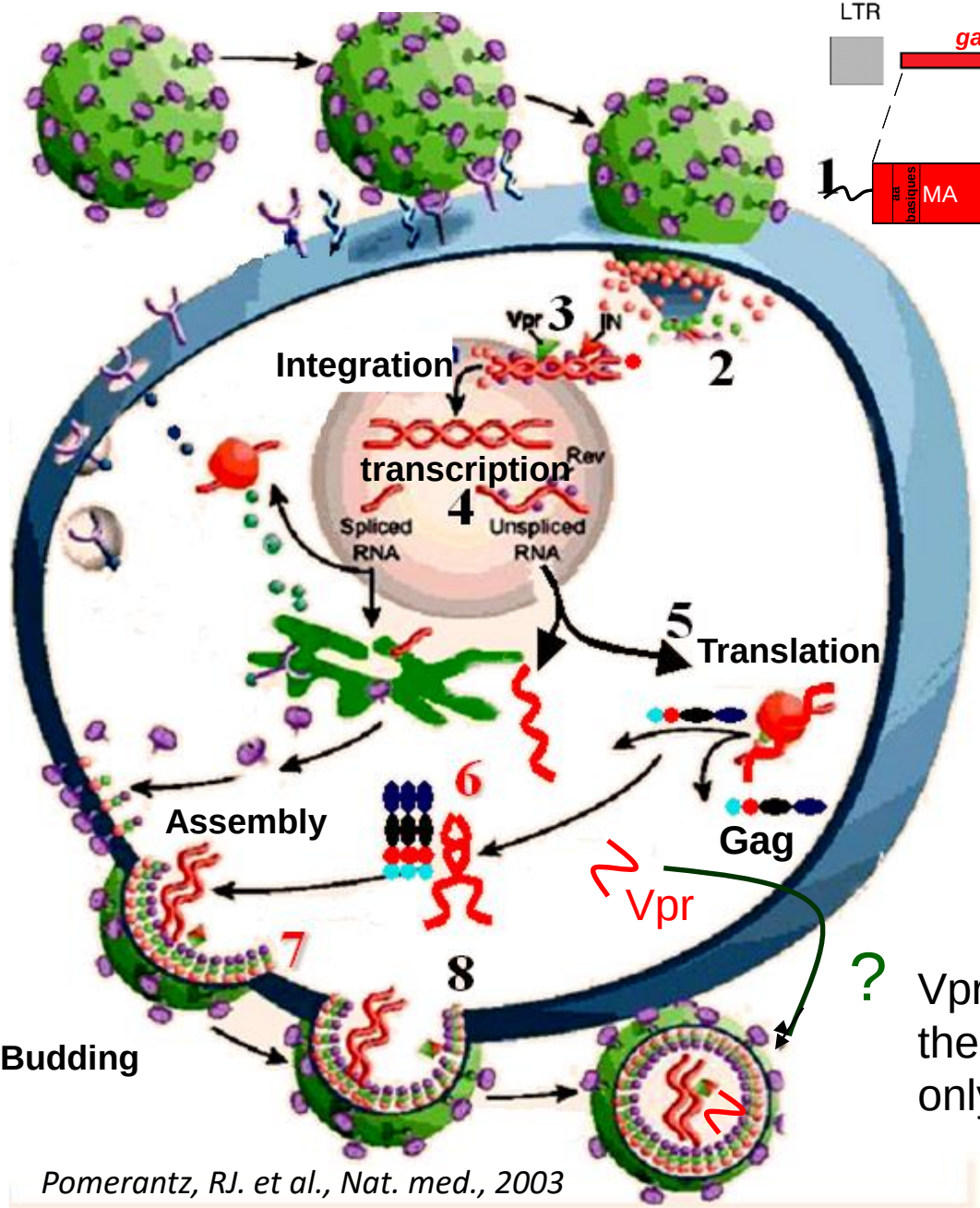

Pomerantz, RJ. et al., Nat. med., 2003

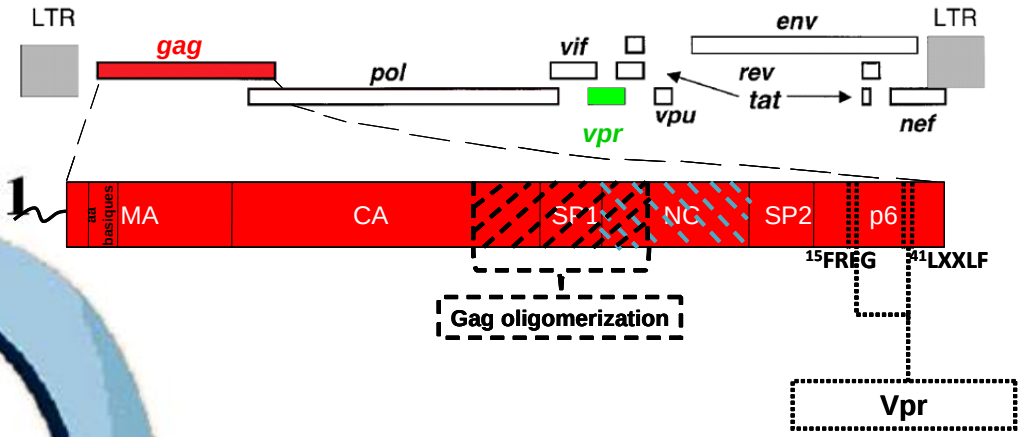

? Vpr is thought to be recruited by Gag in the budding viral particle, but there are only indirect evidences.

Does Vpr directly interacts with Gag?

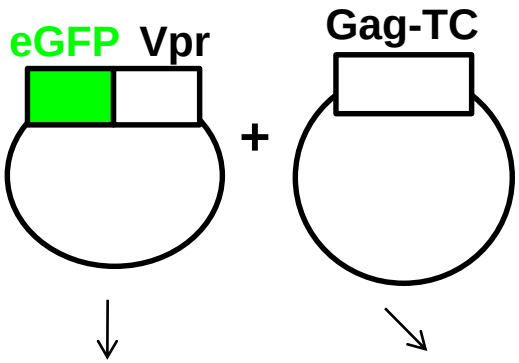

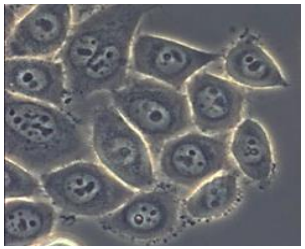

Membrane permeable biarsenical ReAsH dye

Confocal microscopy and FLIM

eGFP-Vpr can be incorporated in viral particles

McDonald D. et al., 2002, J Cell Biol

Forms correctly assembled viral like particles as wtGag

Rudner L. et al., 2005, J Virol

Principle of ReAsH labelling

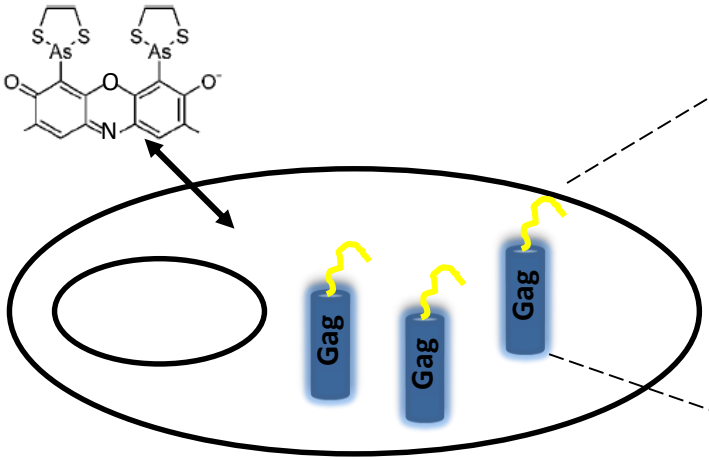

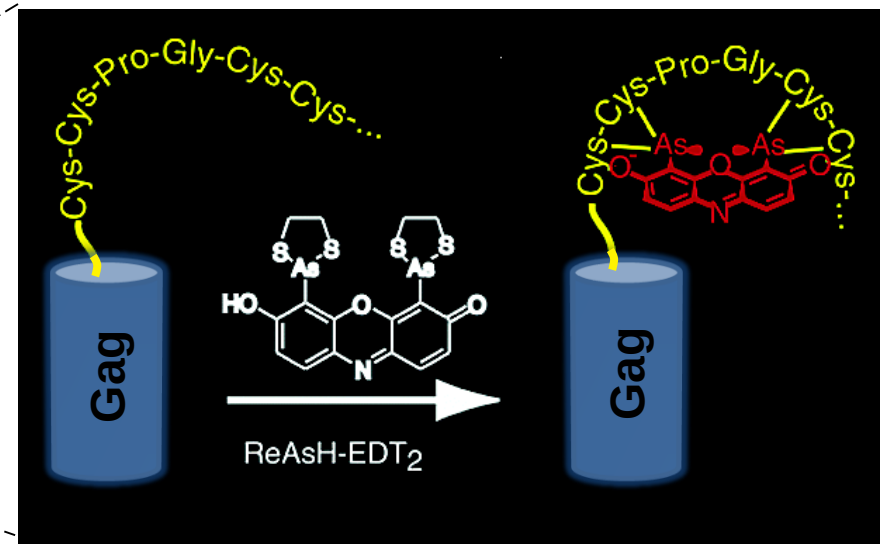

Adams S. et al., 2002, J Am Chem Soc.

Does Vpr directly interact with Gag?

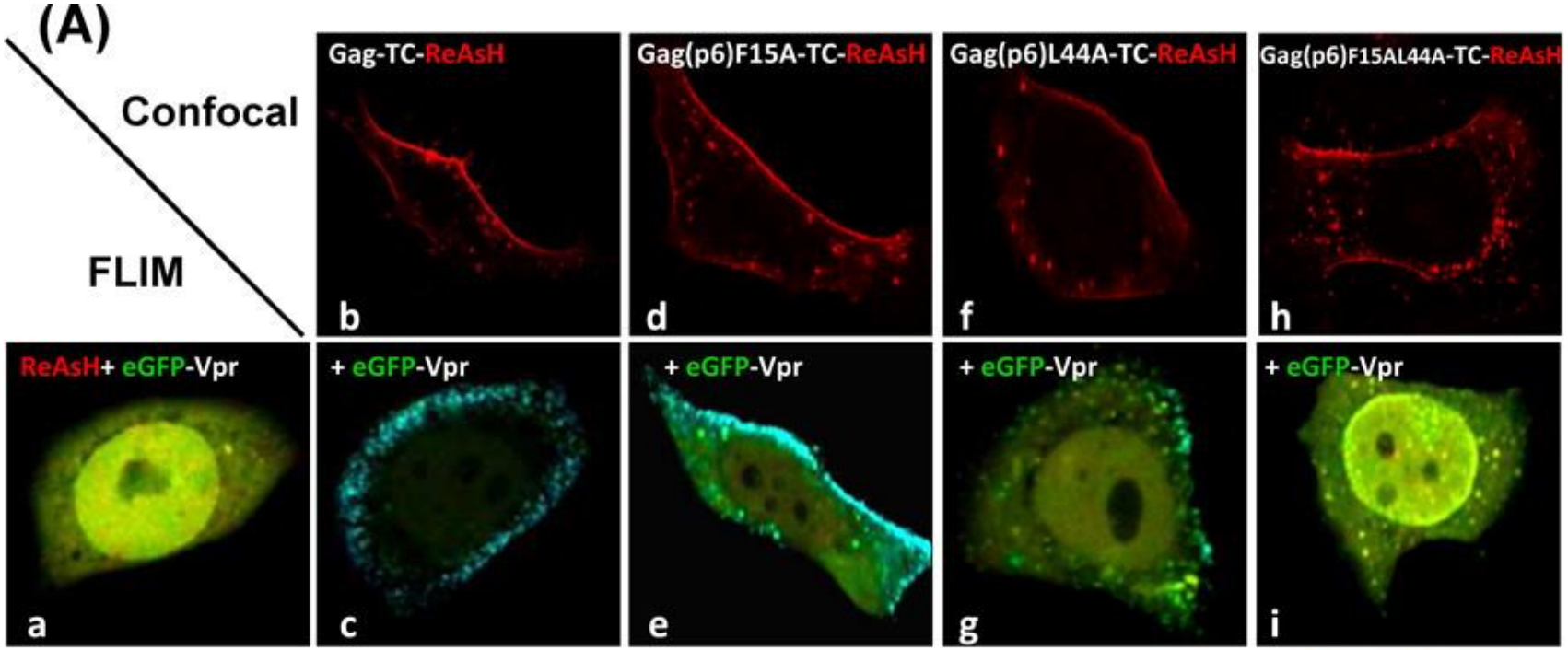

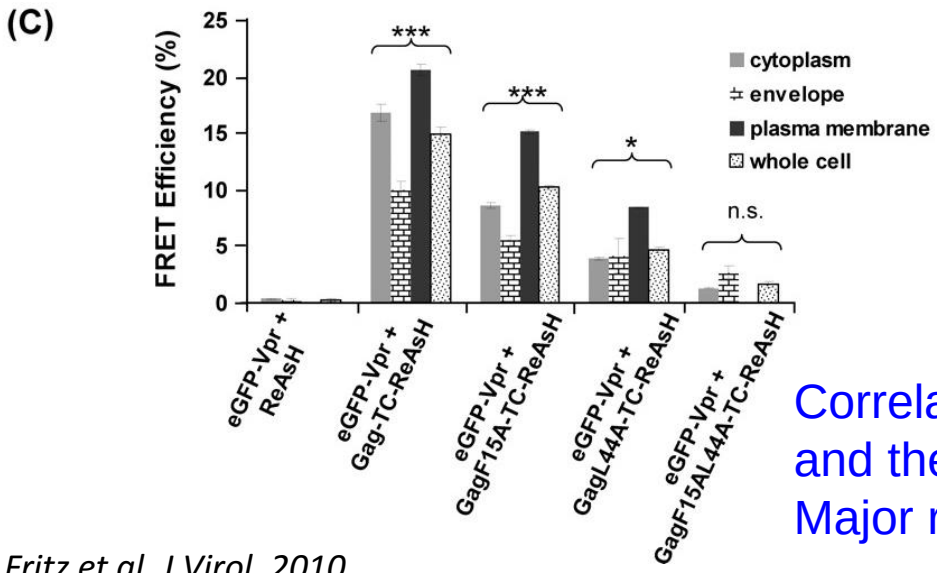

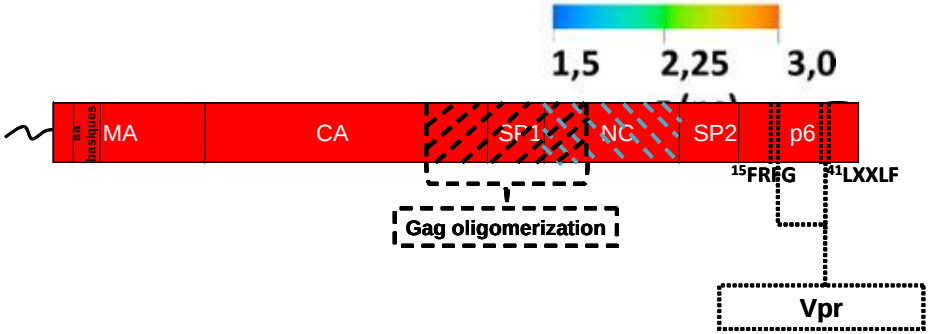

Correlation between the interaction of Gag with Vpr and the accumulation of Vpr at the PM.
Major role of ^{41}LXXLF of Gag for Vpr recognition.

Fritz et al, J Virol, 2010

Is Vpr oligomerization needed for interaction with Gag?

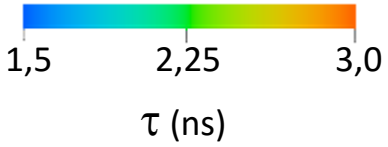

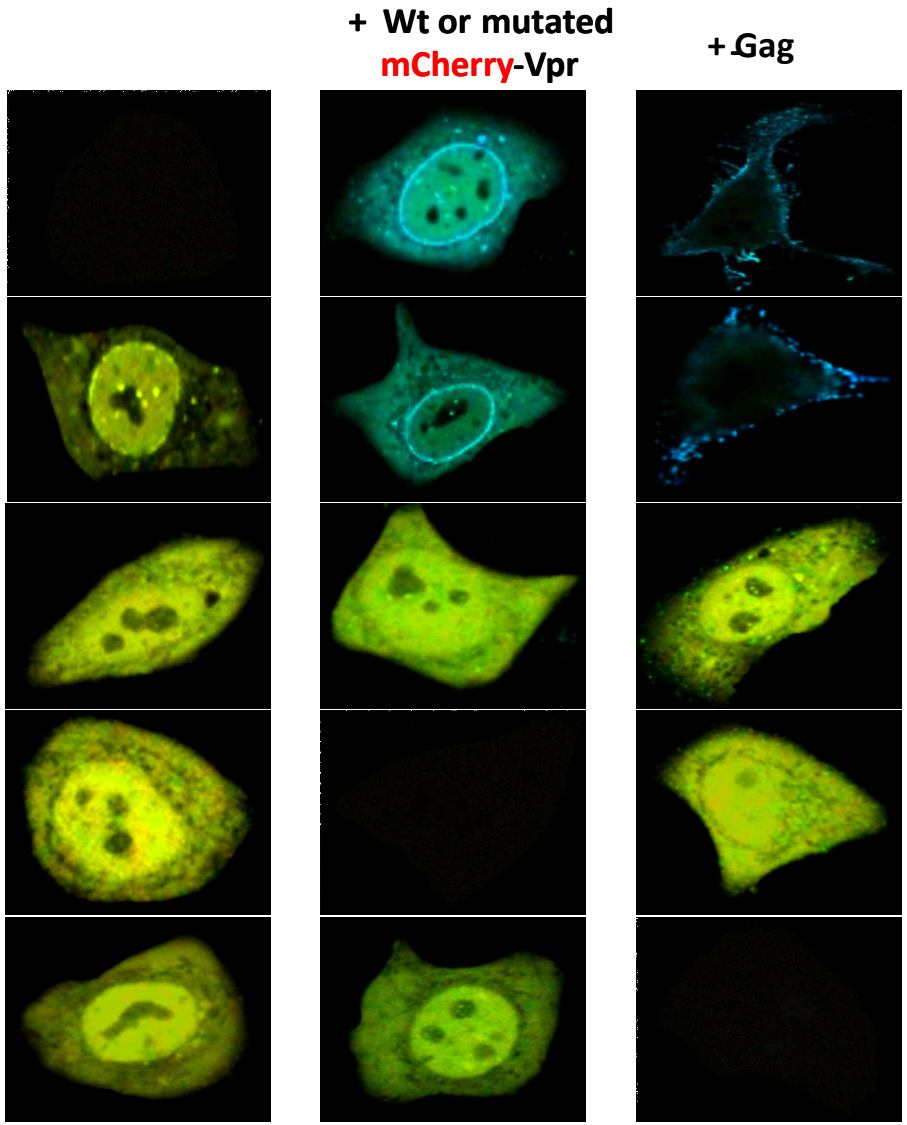

Fritz et al, J Virol, 2010

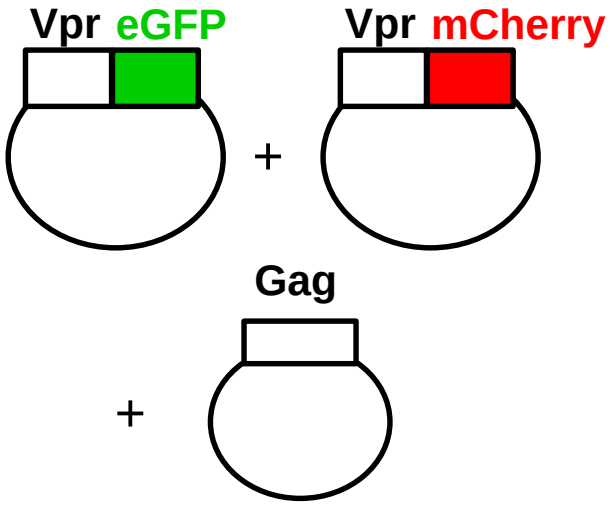

Gag interacts with oligomers at the PM and compacts or rearranges the oligomers.

Vpr oligomerization is required for interaction with Gag.

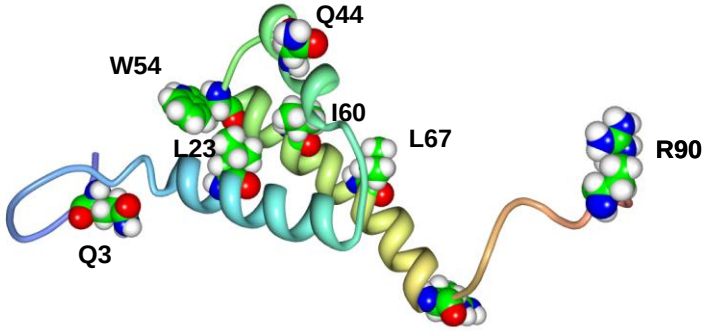

HIV-1 nucleocapsid protein NCp7

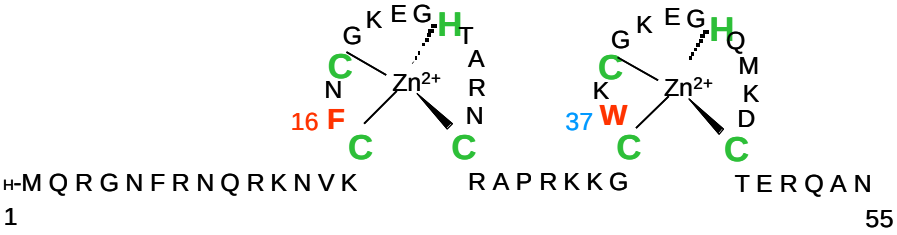

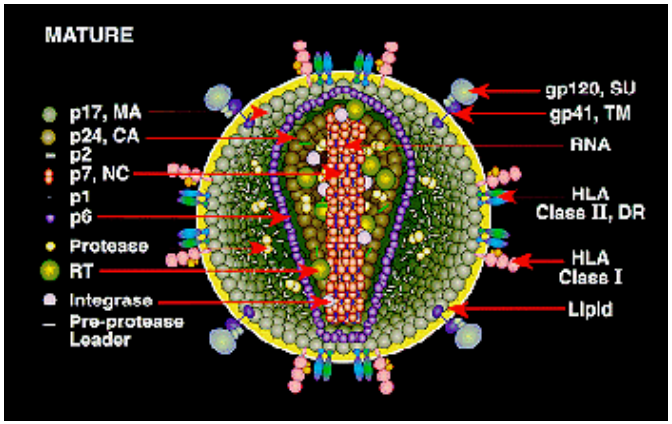

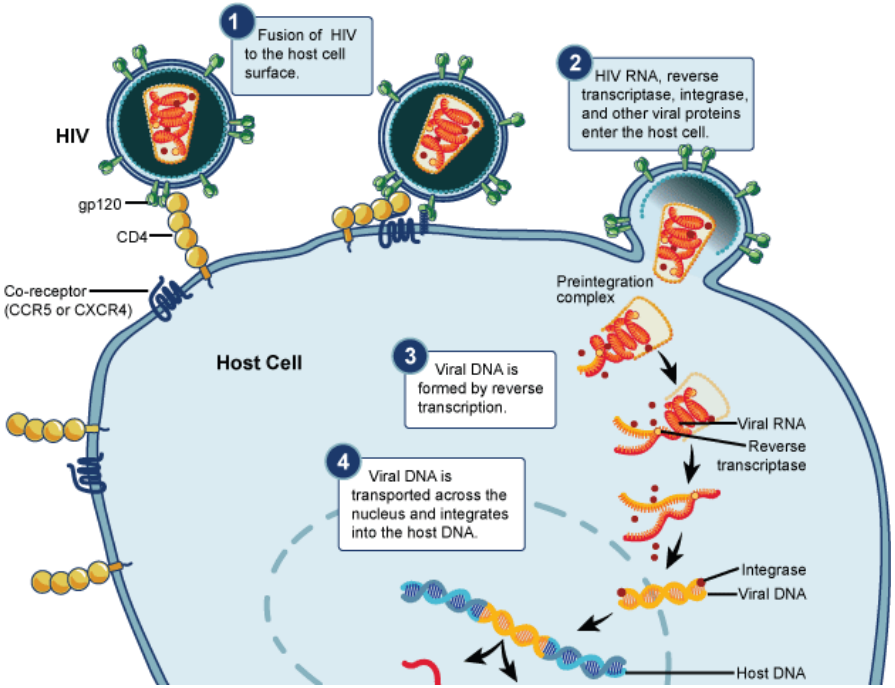

Reverse transcription complex (RTC)

Preintegration complex (PIC)

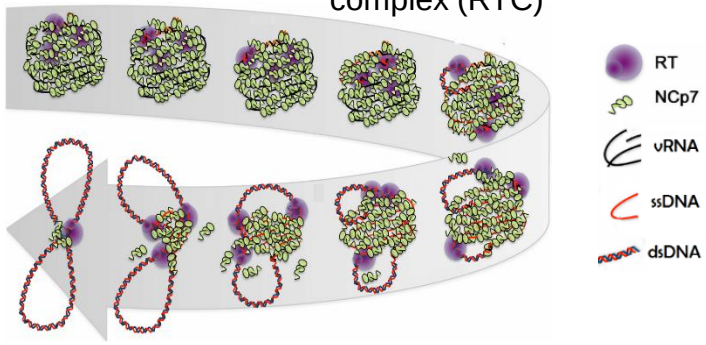

Lyonnais et al.2012

NCp7 binds strongly to ssRNA, but weakly to dsDNA: release in the cytoplasm.

What happens with the released NCp7? What are the cellular partners of NCp7?

Confocal microscopy

HeLa cells transfected with eGFP-labeled NCp7 used as model system

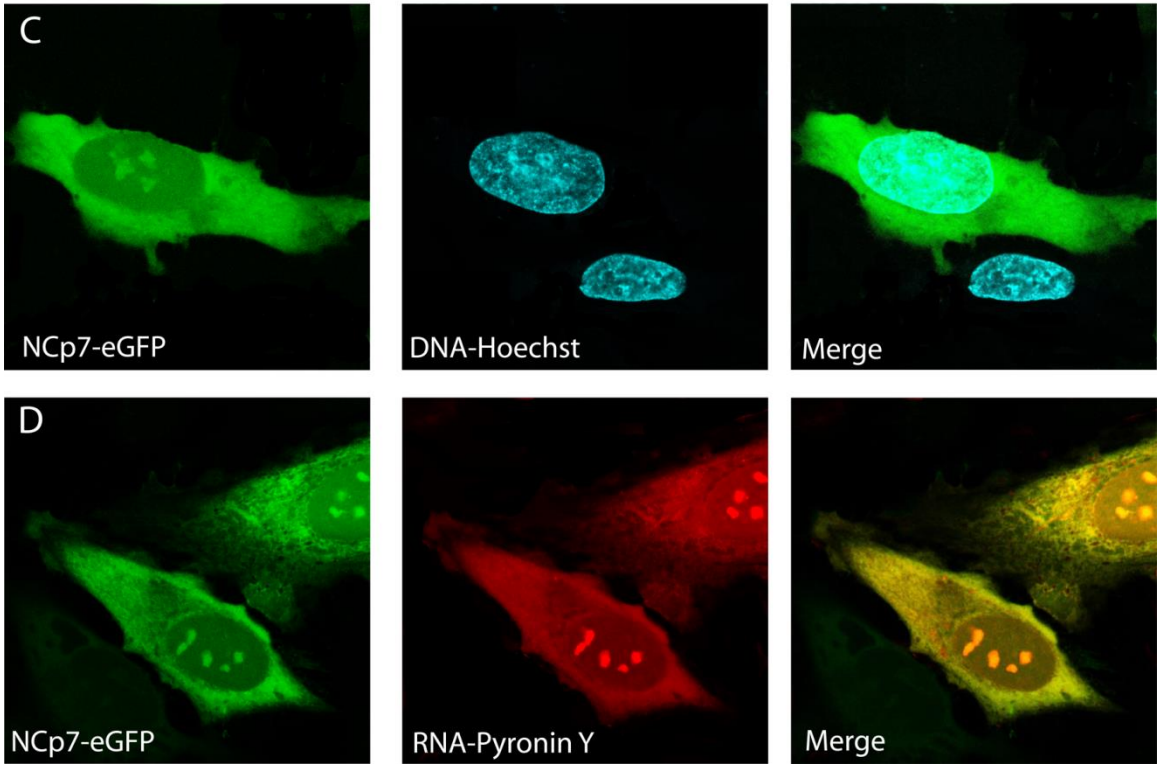

NCp7 is preferentially localized in the cytoplasm and the nucleoli
NCp7 perfectly colocalized with RNAs and to some extent with DNAs

Anton et al, Plos One, 2015

FRET/FLIM

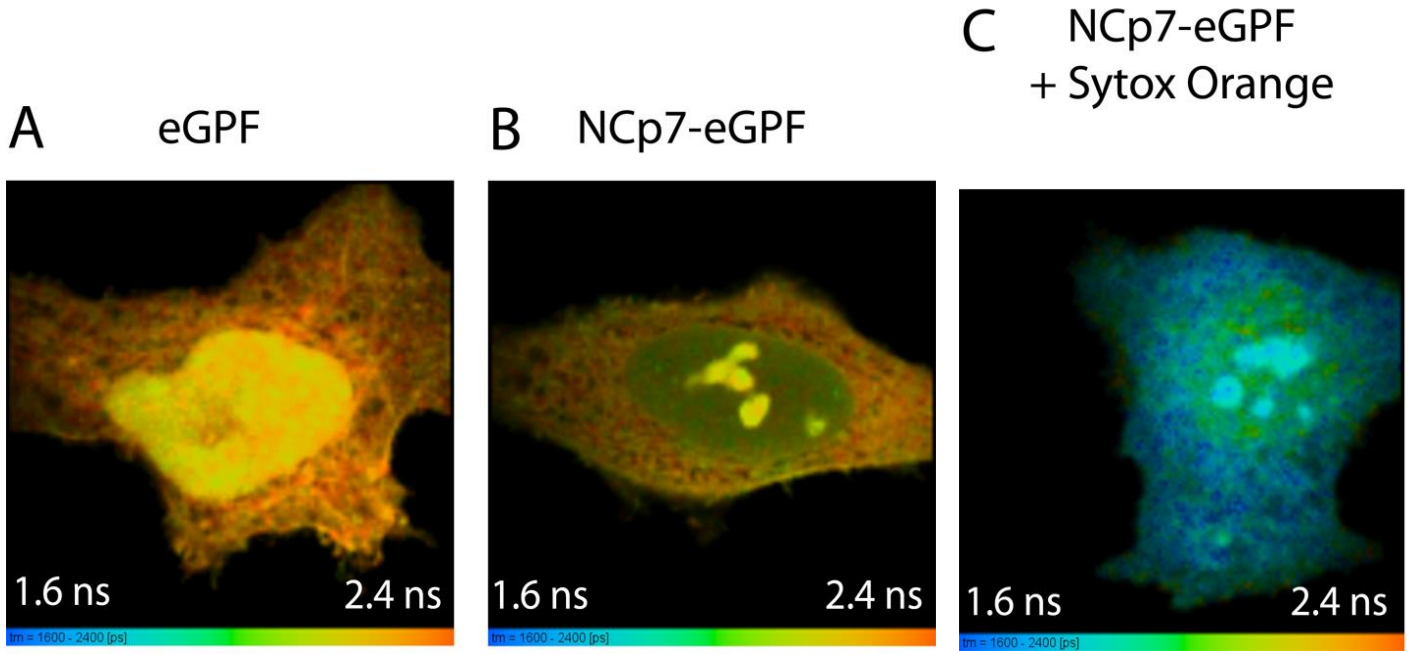

	eGFP	NCp7-eGFP	NCp7-eGFP + Sytox Orange	% FRET
	τ (ns)	τ (ns)	τ (ns)	
Whole cell	2.16±0.01	2.20±0.06	1.75±0.03	**20**
Cytoplasm	2.20 ± 0.02	2.24±0.07	1.69±0.04	**25**
Nucleus	2.11± 0.04	2.11±0.05	1.84±0.04	**13**
Nucleoli	2.0 ± 0.02	2.13±0.07	1.70±0.05	**20**

High FRET (20-25%) in nucleolus and cytoplasm → interaction NCp7/RNAs.
In the nucleoplasm, the lower FRET (13%) suggests that NCp7-eGFP proteins bind less efficiently to DNA as compared to RNA.

FRET/FLIM

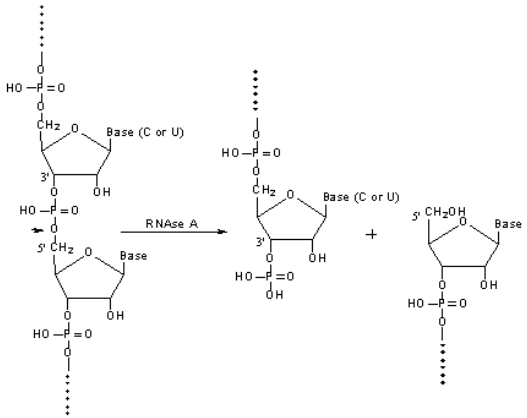

C NCp7-eGPF + Sytox Orange

D NCp7-eGPF + Sytox Orange + RNAse

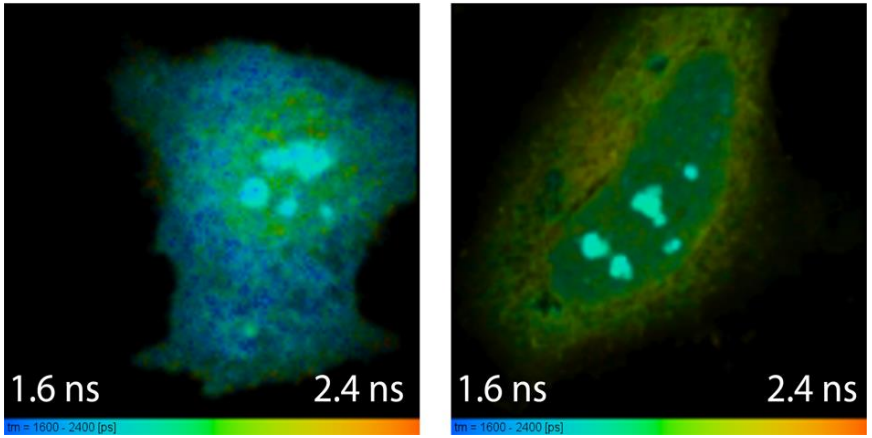

	NCp7-eGFP + Sytox Orange	% **FRET**	NCp7-eGFP + Sytox Orange + RNAse	% **FRET**
	τ (ns)		τ (ns)	
Whole cell	1.75±0.03	**20**	1.99±0.04	**10**
Cytoplasm	1.69±0.04	**25**	1.97±0.03	**12**
Nucleus	1.84±0.04	**13**	1.93±0.05	**8.5**
Nucleoli	1.70±0.05	**20**	1.86±0.05	**13**

Strong decrease with RNase confirms that NCp7 interacts with RNAs in the cytoplasm and the nucleoli.
In the nucleoplasm, the limited FRET decrease may reflect the digestion of nuclear mRNAs.

Cellular RNAs are major partners of NCp7 in the cytoplasm and nucleoli: in line with the 50% of cellular RNA species (in proportion to their cellular level) in HIV-1 particles.

FLIM imaging of 3HFOMe-NC in cells

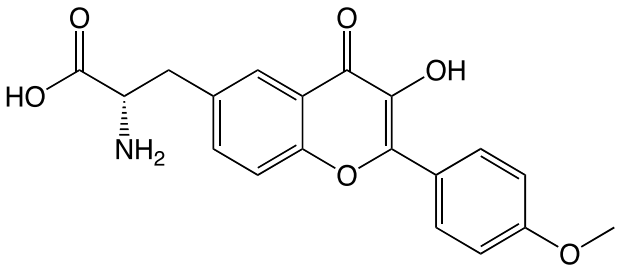

Flavonol-4´-OxyMethyl amino acid (FOMaa)

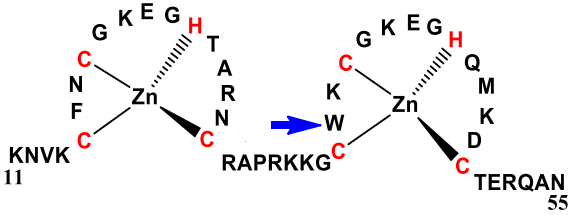

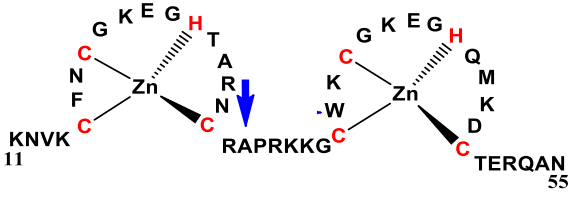

1 Microinjection of the labeled peptide inside the cell

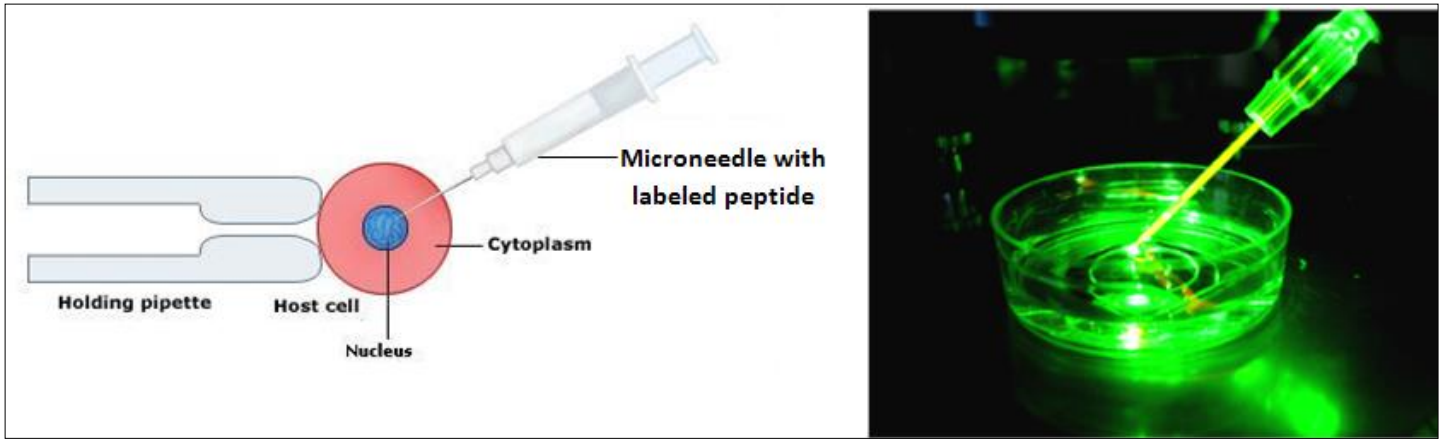

2 FLIM imaging of HeLa cells injected with labelled peptides

Sholokh et al, J Phys Chem B, 2015

FLIM imaging of NC-W37-M3HFaa in cells

NC-W37-M3HFaa

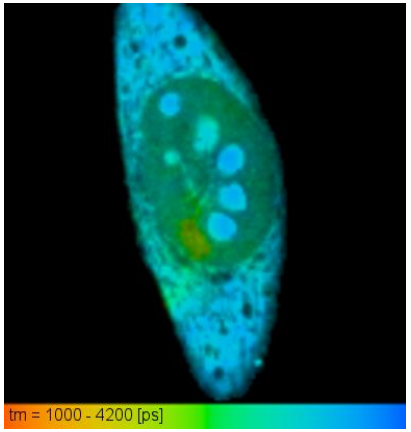

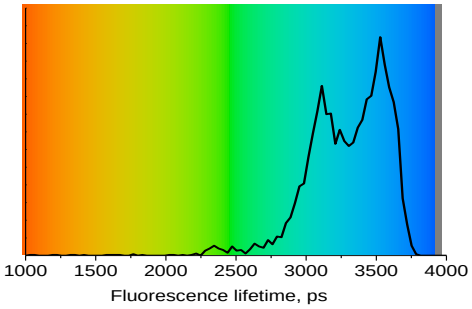

Nucleoli: 3.7-4.3 ns
Cytoplasm: 3.8-4.0 ns
Nucleoplasm: 3.2-3.6 ns

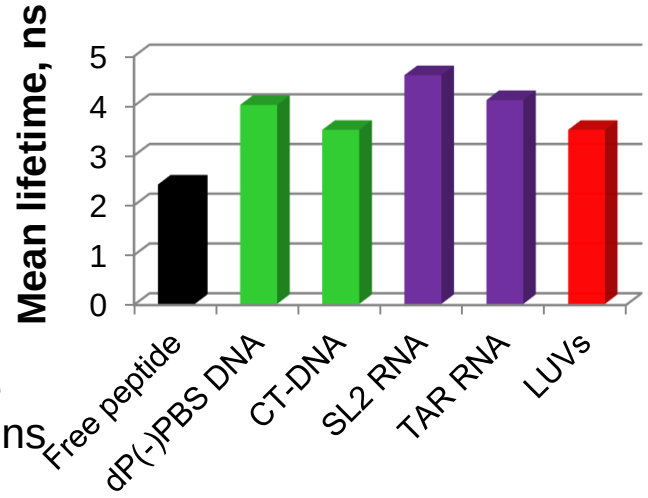

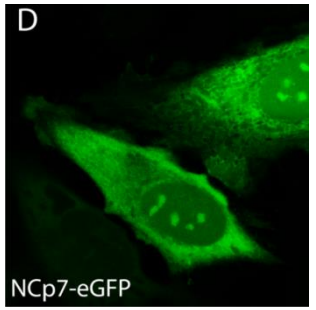

NC-A30-M3HFaa

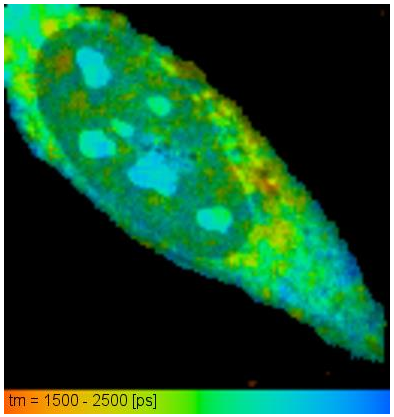

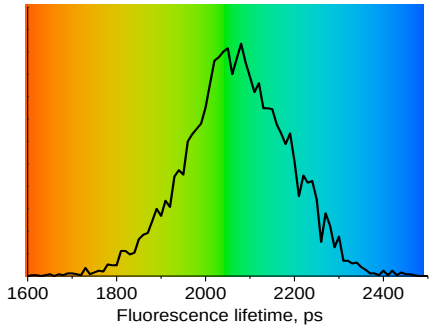

Nucleoli: 2.4-2.6 ns
Cytoplasm: 2.2-2.4 ns
Nucleoplasm: 2.2-2.3 ns

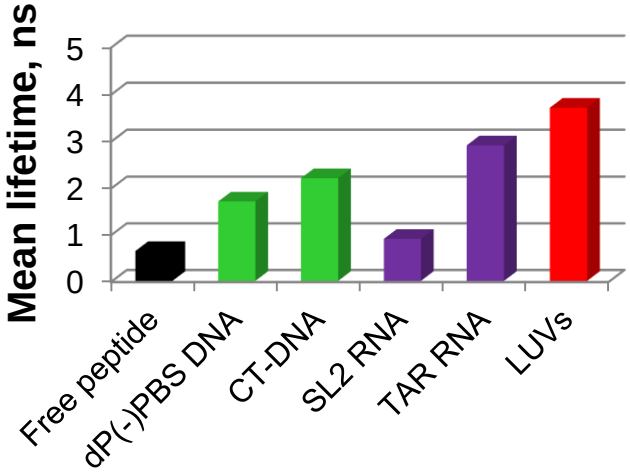

No free NCp7 can be observed. Binding to lipids seems limited. NCp7 binds to RNA in nucleoli and the cytoplasm. In nucleus, low binding to DNA

Intracellular dynamics of NCp7: FCS

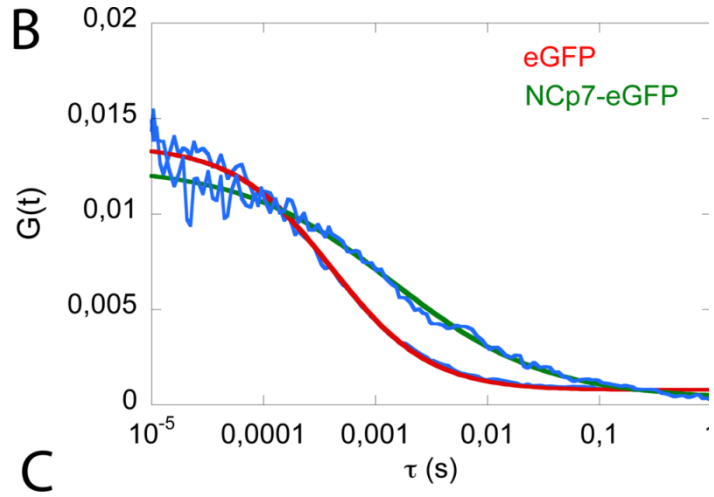

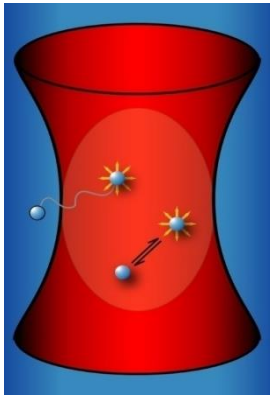

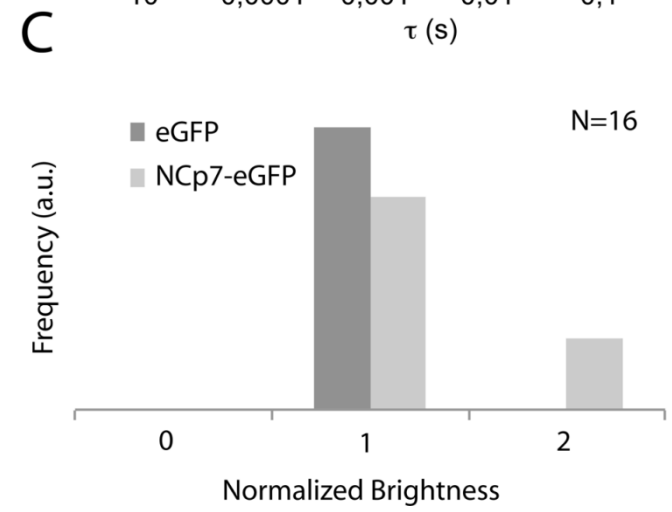

Cytoplasm				Nucleus	
		D (µm²/s)	α	D (µm²/s)	α
FCS	eGFP	34 ± 3	0.92 ± 0.08	31 ± 1	0.95 ± 0.09
	NCp7-eGFP	4.5 ± 1	0.65 ± 0.03	7 ± 3	0.60 ± 0.09

- D_{eGFP} = 6-8 × $D_{NCp7\text{-}eGFP}$ confirmed that NCp7-eGFP molecules diffuse in large complexes.
- $\alpha \sim 1$ for eGFP (free diffusion).
- α = 0.60-0.65 for NCp7-eGFP→ motion of the NCp7-complexes in obstructed environment.

Brightness analysis → complexes do not contain more than two NCp7-eGFP molecules, excluding that they correspond to high molecular weight NCp7-eGFP aggregates

Intracellular dynamics of NC: RICS

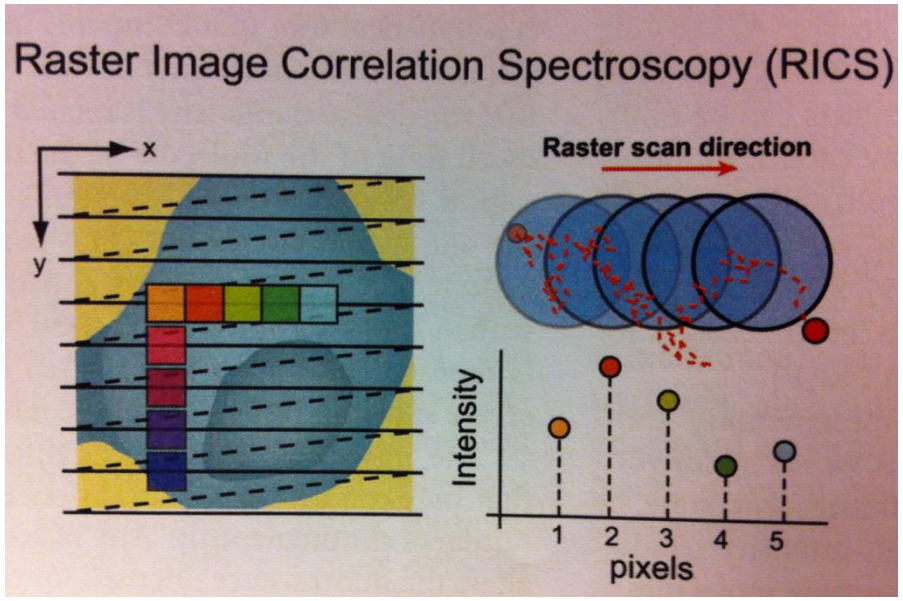

RICS analyses the fluorescence intensity fluctuations between neighboring pixels by spatially autocorrelating the image in x and y directions

Raster Scanned Image

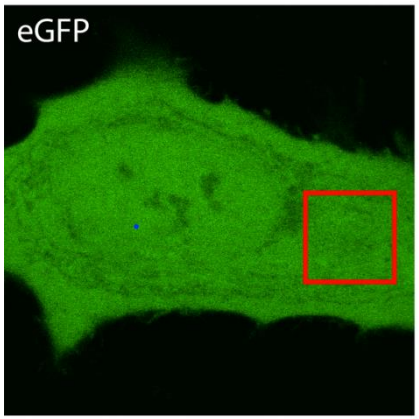

$$G_s(\xi,\psi)=\frac{\langle I(x,y)I(x+\xi,y+\psi)\rangle_{x,y}}{\langle I(x,y)\rangle^2_{x,y}}$$

Spatial Correlation surface

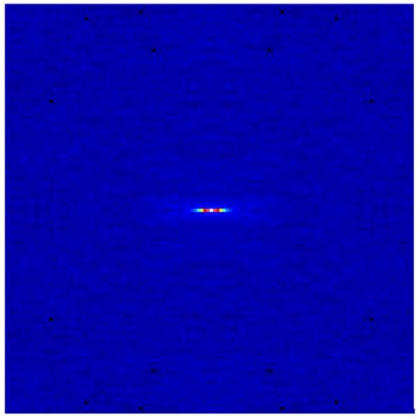

$$G_{RICS}(\xi,\Psi)= S(\xi,\Psi)\times G(\xi,\Psi)$$

Fitting function

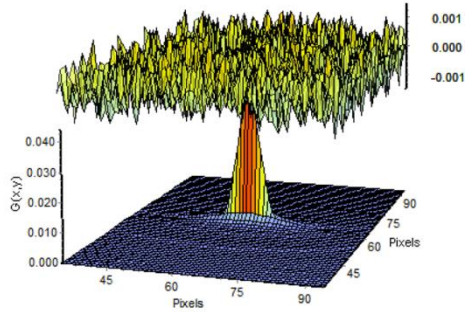

$$S(\xi,\Psi)=\exp\left(-\frac{\left[\left(\frac{2\xi\delta r}{w_0}\right)^2+\left(\frac{2\Psi\delta r}{w_0}\right)^2\right]}{\left(1+\frac{4D\left(\tau_p\xi+\tau_l\Psi\right)}{w_0^2}\right)}\right)$$

$$G(\xi,\Psi)=\frac{\gamma}{N}\left(1+\frac{4D\left(\tau_p\xi+\tau_l\Psi\right)}{w_0^2}\right)^{-1}\left(1+\frac{4D\left(\tau_p\xi+\tau_l\Psi\right)}{w_z^2}\right)^{-\frac{1}{2}}$$

Intracellular dynamics of NC: RICS

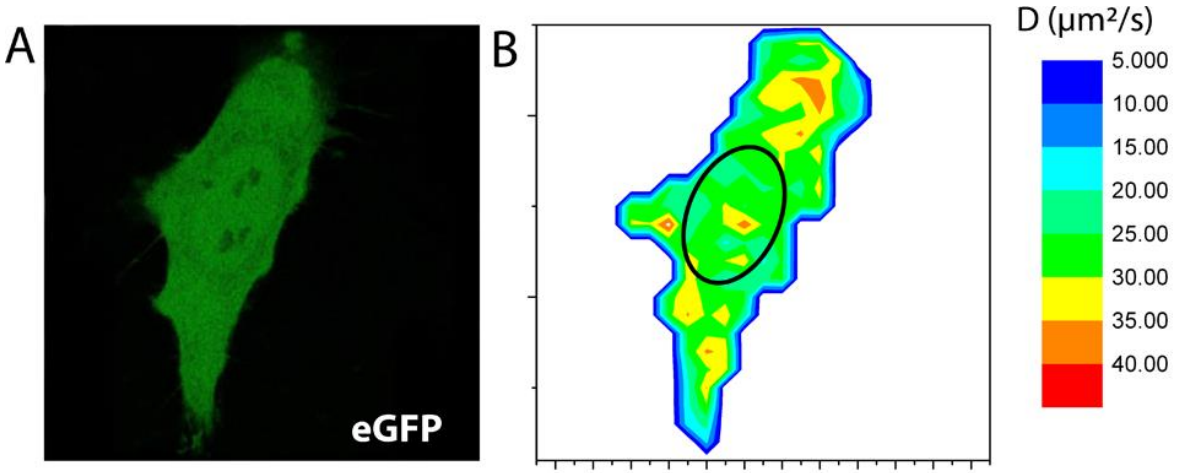

D values calculated in windows of 64x64 pixels

For eGFP, the distribution of D values was homogeneous all over the cell (25-35 µm²/s)

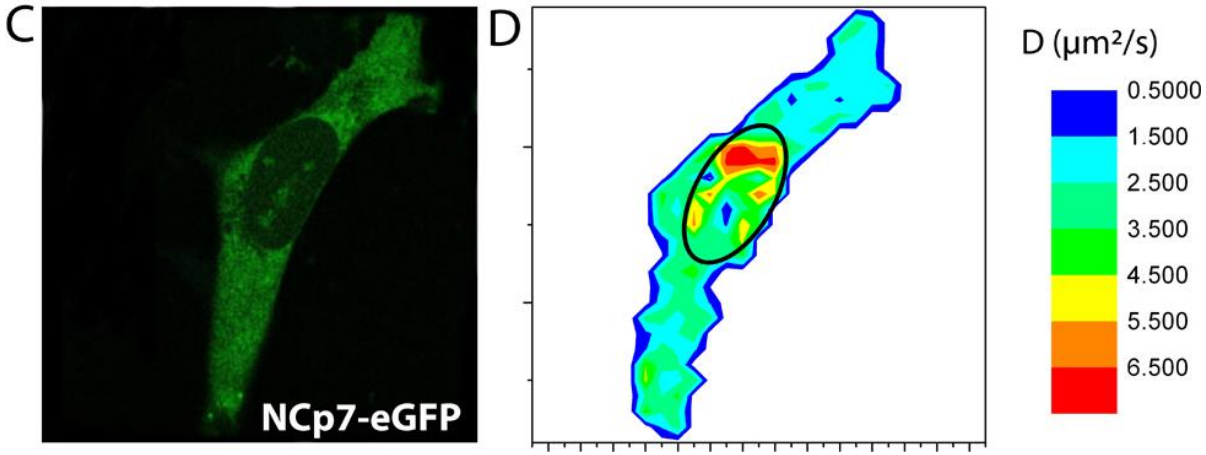

For NCp7-eGFP, D values (1.5-4 µm²/s) homogeneously distributed in the cytoplasm.

Diffusion in nucleus is faster (3.5-6.5 µm²/s).

Intracellular dynamics of NC: RICS

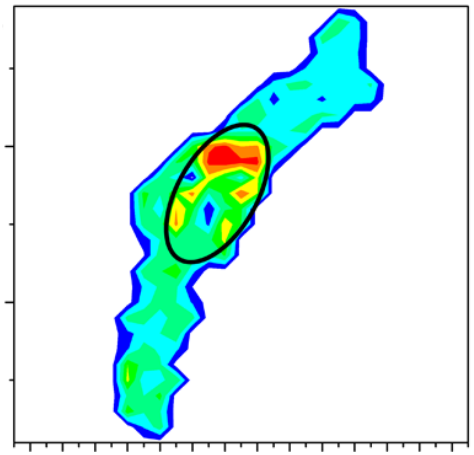

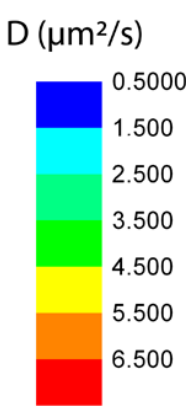

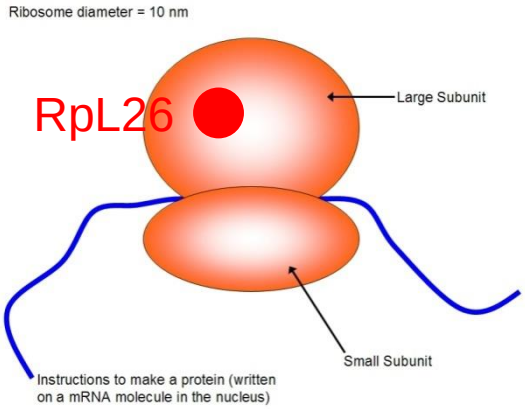

Ribosomal RNAs represent about 80% of the total RNA in HeLa cells

D (~0.5 µm²/s) in the nucleoli: NCp7-eGFP form larger complexes or these complexes are slowed down by the dense and compact environment of the nucleoli.

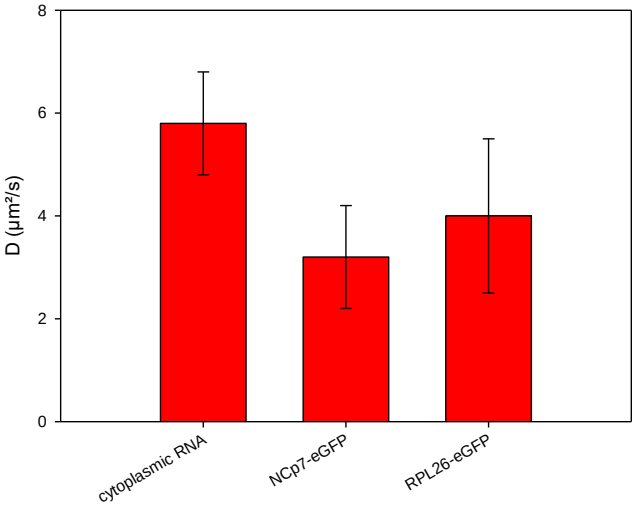

NCp7-eGFP does not bind randomly to cellular RNAs but prefers large RNA molecules or ribonucleoprotein complexes.

D values of RpL26-eGFP and NCp7-eGFP are close → NCp7 may bind RNAs in ribosomes

Intracellular dynamics of NC: FCCS

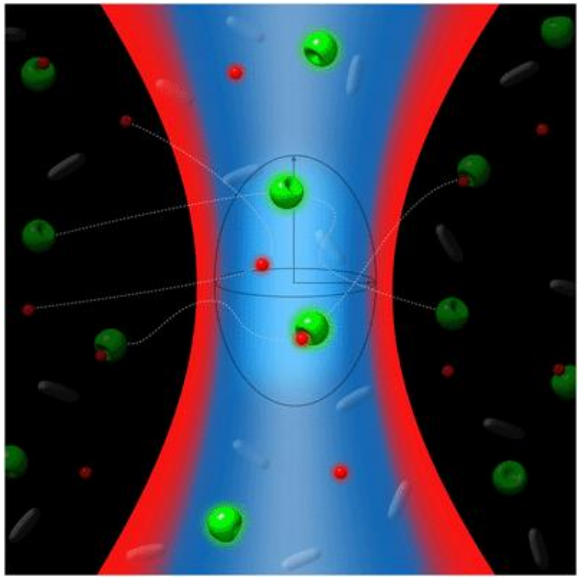

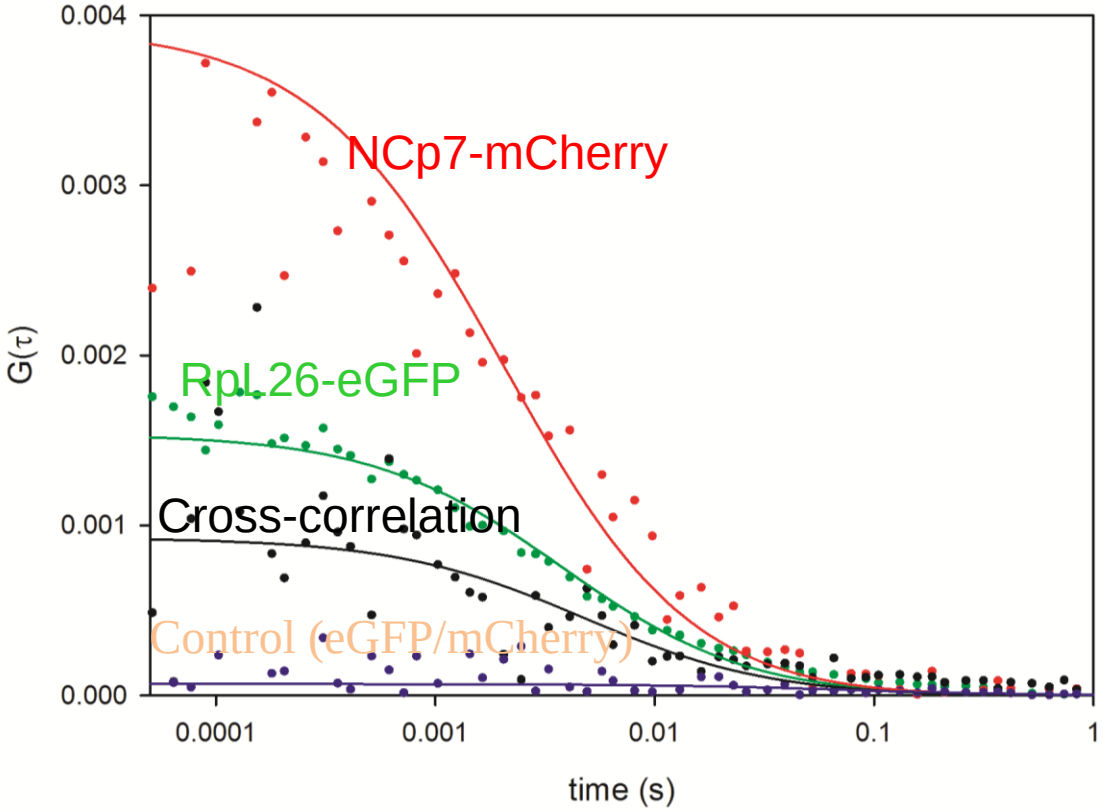

FCCS correlates the temporal fluorescence fluctuations of two differently labeled molecules diffusing through the focal volume.

RpL26 (5.6 (± 0.7) $\mu m^2/s$), NCp7-mCherry (6 (± 3) $\mu m^2/s$) and FCCS (4 (± 3) $\mu m^2/s$), fully consistent with the D values measured by RICS

FCCS confirms that NCp7 and RpL26 diffuse together in the cytoplasm within the same ribosomic complex

Evidence of the overlap between the epitopes of monoclonal antibodies (Mab) against poliovirus type 3

Binding affinity of Mab by SPR

Virus strain	Mab	K_D (pM)
Saukett (type 3)	1E3-3G4	54
Saukett (type 3)	4B7-1H8	189
Saukett (type 3)	4H8-3A12	102

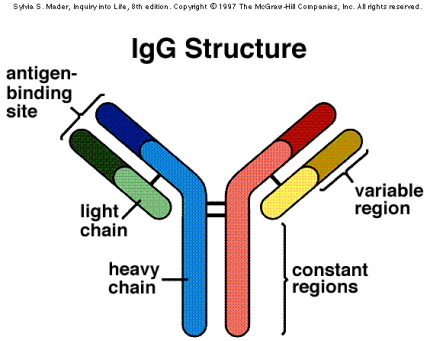

Contact areas between Fabs and poliovirus type 3 surface structure

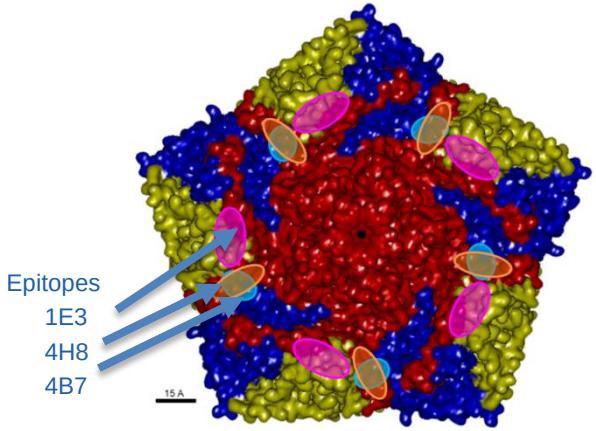

CryoEM structures of Type 3 Polio Virus in the free form (a) or complexed to Fab 4H8-3A12 (b), Fab 1E3-3G4 (c) or Fab 4B7-1H8 (d).

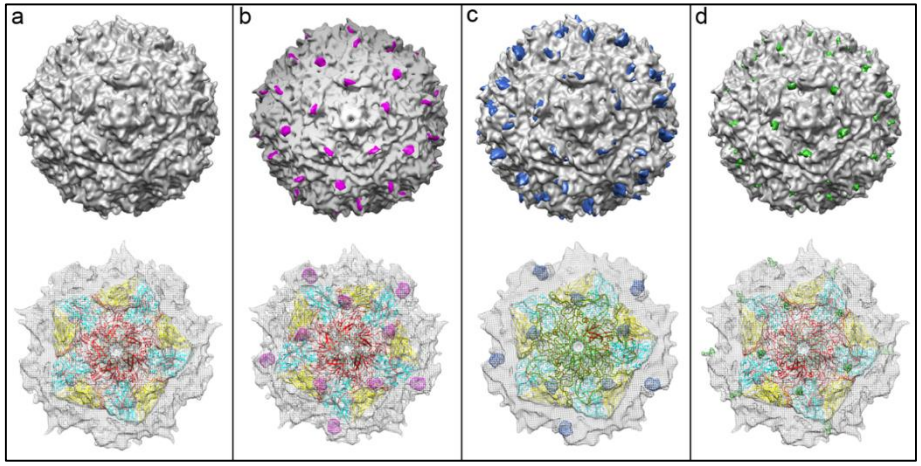

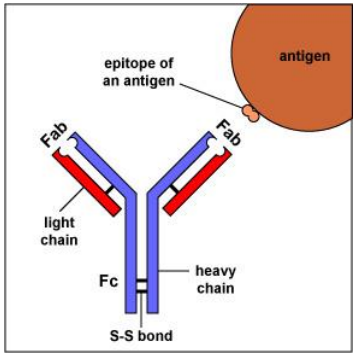

Capsid composed of 60 copies of 4 different polypeptides (~30 nm of diameter)

Could FCS be used to detect competition between corresponding Mabs for overlapping epitopes?

Richert et al, Mabs, 2016

Evidence of the overlap between the epitopes of Mabs

Binding of Mabs to poliovirus particles, as monitored by FCS

Raw curves

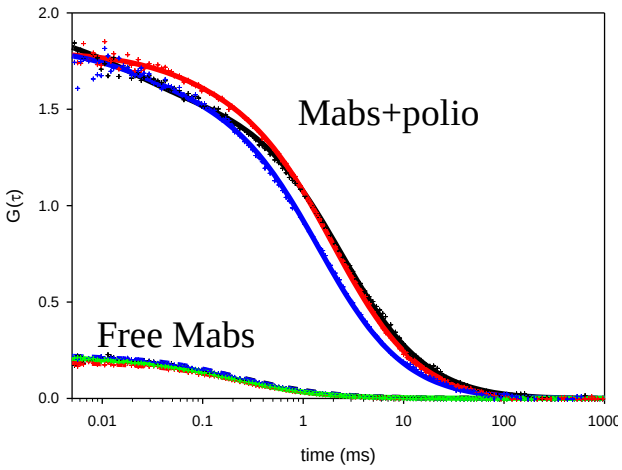

Normalized curves

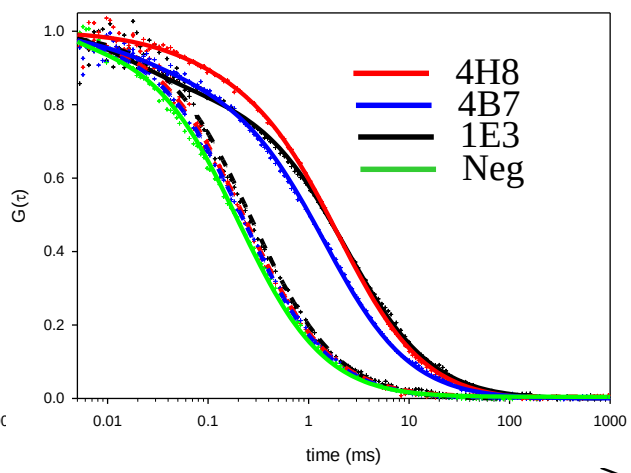

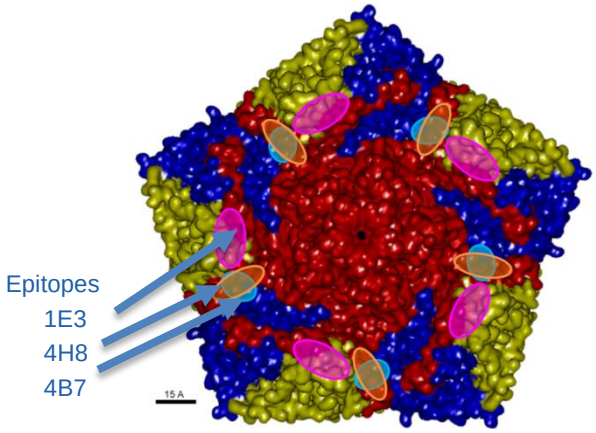

	Free Mabs		Poliovirus + Mabs (ratio 1/10)	
MAbs	Diffusion coefficients ($\mu m^2.s^{-1}$)*	Hydrodynamic radius (nm)	Diffusion coefficients ($\mu m^2.s^{-1}$)*	Hydrodynamic radius (nm)
1E3-3G4	57 ± 3	3.8± 0.4	12 ± 2	17 ± 3
4H8-3A12	58 ± 8	3.7± 0.6	16 ± 4	13± 5
4B7-1H8	60 ± 3	3.6± 0.4	12 ± 4	17± 5
Negative Mab	61 ± 8	3.5 ± 0.6	50 ± 20	4.3±1.2

Binding of Alexa488-labeled Mabs to the viral particles could be monitored by FCS

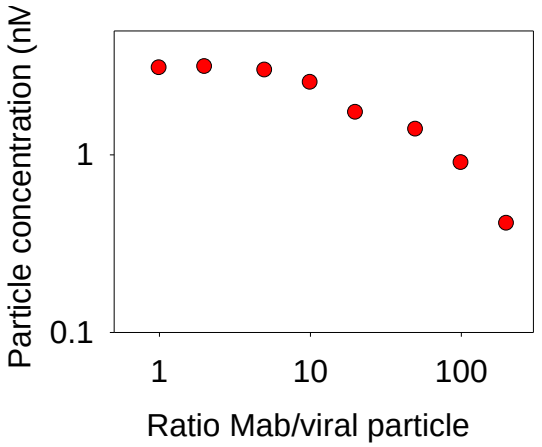

Concentration of viral particles could be determined at low Mab/particle ratio. Aggregation at a ratio > 30, due to presence of two binding sites per Mab

Evidence of the overlap between the epitopes of Mabs

Competition with Mab 4H8

Raw curves

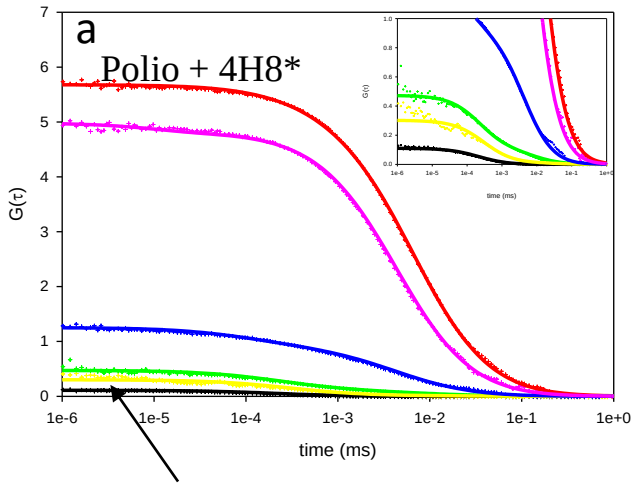

Normalized curves

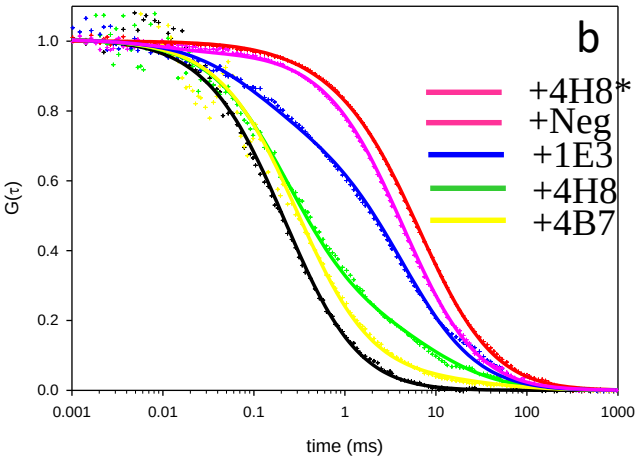

Polio/4H8*/X: 1/10/20

strong competition:

- with non labeled 4H8 → the number of Mabs that can bind to the virus << 60
- With non labeled 4B7 → strong overlap of epitopes

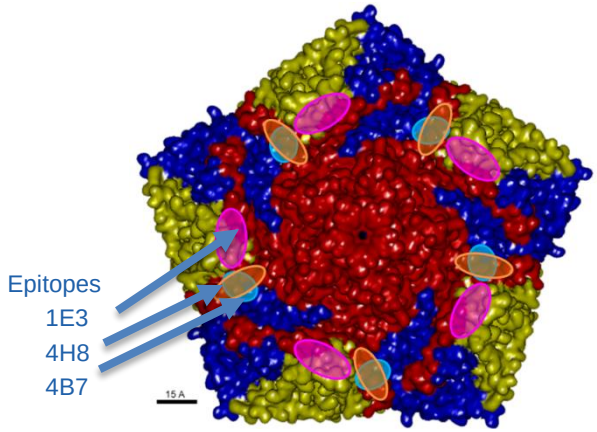

Significant competition (22% of 4H8 remains bound) with non labeled 1E3 → decreases the access of 4H8 to its epitope

Evidence of the overlap between the epitopes of Mabs

Competition with Mab 4B7

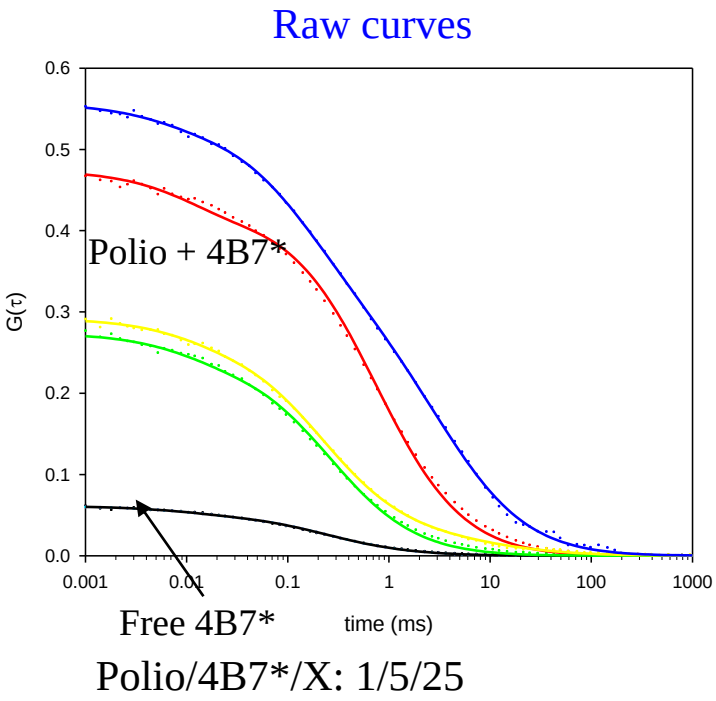

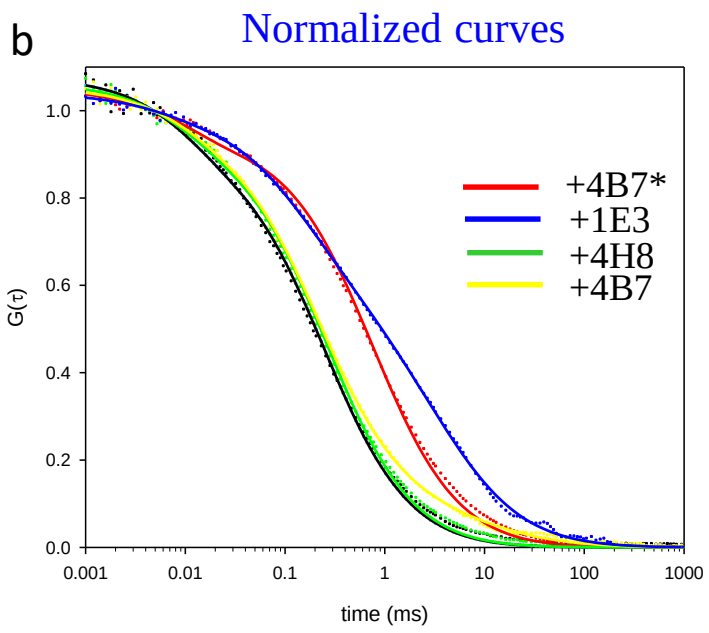

strong competition with non labeled 4B7 and 4H8 (10% of 4B7* remains bound) → strong overlap of epitopes

Marginal competition with non labeled 1E3 → marginal overlap of 4B7 and 1E3 epitopes

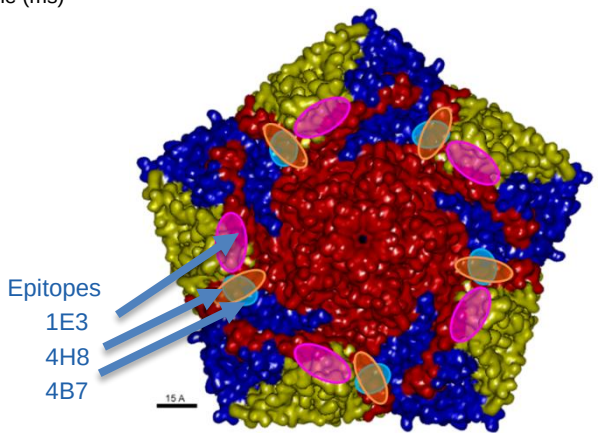

Evidence of the overlap between the epitopes of Mabs

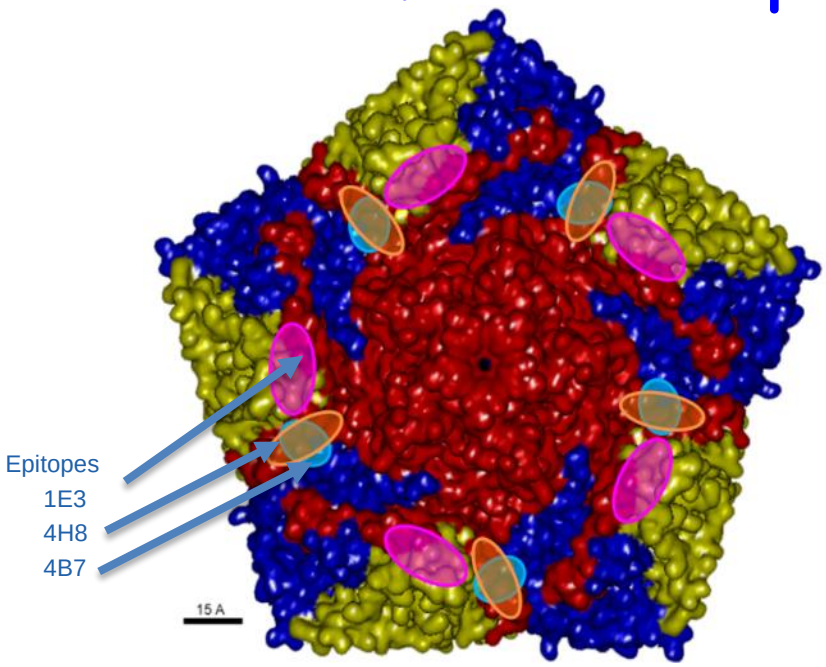

Strong competition between MAbs 4B7 and 4H8 due to strong overlap of their epitopes that share the same VP1 loop.

Significant competition between MAbs 4H8 and 1E3, and marginal competition between MAbs 4B7 and 1E3 → MAbs 4H8 and 4B7 bind in a different orientation to their epitopes, so that only the former sterically clashes with MAb 1E3 bound to its epitope.

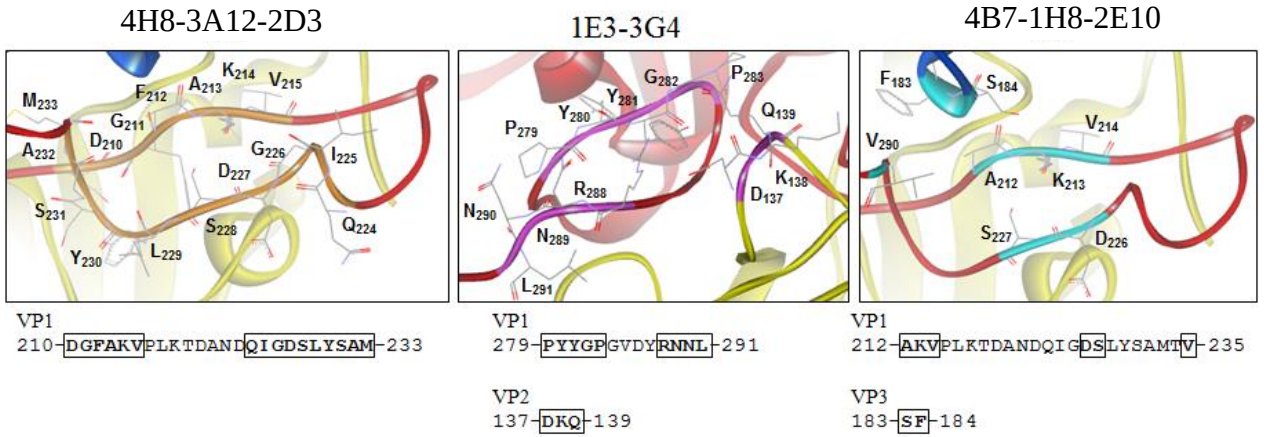

FCS constitutes a unique tool for assessing epitope overlap between MAbs raised against a viral particle.

Conclusions

FLIM-FRET approach allows discriminating monomers from small or large oligomers and monitoring their spatio-temporal distribution in cells.

Number of protomers in an oligomers is ideally assessed by FCS

FLIM-FRET allows monitoring protein-protein as well as protein-nucleic acid interactions.

FCS is a powerful technique to evidence overlaps of mAbs on viral particles

Acknowledgements

- Halina Anton, Sarwat Zgeib, Iryna Lysova, Pascal Didier, Ludovic Richert, Marianna Sholokh, Hugues de Rocquigny, Eleonore Réal, Emmanuel Boutant, Alex Glushonkov
-CNRS, ANR, FP7 Thinpad project, ANRS, ARCUS, DNIPRO

METHODS AND APPLICATIONS IN FLUORESCENCE

Editors-in-Chief

David Birch Otto Wolfbeis Yves Mely

First impact factor: 2.43

Do not hesitate to submit your work!

Accepting submissions at iopscience.org/maf